

RESEARCH ARTICLE

Subspecies differences in thermal acclimation of mitochondrial function and the role of uncoupling proteins in killifish

Heather J. Bryant*, Dillon J. Chung and Patricia M. Schulte

ABSTRACT

Thermal effects on mitochondrial efficiency and ATP production can influence whole-animal thermal tolerance and performance. Thus, organisms may have the capacity to alter mitochondrial processes through acclimation or adaptation to mitigate these effects. One possible mechanism is through the action of uncoupling proteins (UCPs), which can decrease the proton-motive force independent of the production of ATP. To test this hypothesis, we examined the mRNA expression patterns of UCP isoforms and characterized the effects of thermal acclimation and putative local thermal adaptation on mitochondrial capacity, proton leak and P/O ratios in two subspecies of Atlantic killifish (*Fundulus heteroclitus*). *Ucp1* was the dominant isoform in liver and was more highly expressed in northern killifish. We found that cold acclimation increased mitochondrial capacity (state III and maximum substrate oxidation capacity), state II membrane potential, proton leak and P/O ratios in northern, but not southern, killifish liver mitochondria. Palmitate-induced mitochondrial uncoupling was detected in northern, but not southern, killifish liver mitochondria, consistent with the differences in *Ucp* mRNA expression between the subspecies. Taken together, our data suggest that mitochondrial function is more plastic in response to thermal acclimation in northern killifish than in southern killifish and that UCP1 may play a role in regulating the proton-motive force in northern, but not southern, killifish in response to thermal acclimation. These data demonstrate the potential for adaptive variation in mitochondrial plasticity in response to cold.

KEY WORDS: *Fundulus heteroclitus*, Temperature, Mitochondria, Fish, UCP, Adaptation

INTRODUCTION

Environmental temperature is an important factor that influences the geographic distribution of ectotherms owing to its effects on biochemical reaction rates which, in turn, affect whole-animal performance (Hochachka and Somero, 2002; Chung and Schulte, 2015; Fanguie et al., 2009b; Iftikar and Hickey, 2013; Pörtner, 2001). Because of their key role in providing the majority of the ATP needed for cellular processes, mitochondria are suggested to be an important determinant of these responses of animals to changes in environmental temperature (Iftikar and Hickey, 2013; Pörtner, 2001). Many studies have examined the effects of thermal acclimation or adaptation on mitochondrial respiratory capacity

(e.g. Chung and Schulte, 2015; Chung et al., 2017, 2018; Fanguie et al., 2009b; Abele et al., 2002; Dahlhoff and Somero, 1993; Guderley and Johnston, 1996; Strobel et al., 2013; Lannig et al., 2005; Kraffe et al., 2007), but mitochondrial efficiency and proton leak have also been suggested to be crucial parameters influencing organismal responses to temperature (e.g. Salin et al., 2015; Trzcionka et al., 2008).

Measures of non-ADP-phosphorylating (e.g. state IV) respiration rates or respiratory control ratios (RCRs; state III/state IV) are often utilized to estimate mitochondrial leak and efficiency, respectively. A variety of studies in fish suggest that state IV respiration increases with decreasing acclimation temperature, with little or no effect on RCR (dos Santos et al., 2013a; Chung and Schulte, 2015; Chung et al., 2018), representing partial or complete compensation for the effects of low temperature on enzyme activity and the physical state of the inner mitochondrial membrane (IMM) (e.g. Chung and Schulte, 2015; Guderley, 1990). However, other studies have detected increases in RCR with decreases in acclimation temperature (Lannig et al., 2005; van den Thillart and Modderkolk, 1978; Moyes et al., 1988; Guderley and Johnston, 1996). One possible reason for the variety of observed effects of temperature on mitochondrial proton leak and efficiency may be variation among species in the strategies pursued (e.g. cold compensation versus low temperature dormancy). Alternatively, the technical limitations associated with interpreting state IV measurements and coupling ratios as representing measures of mitochondrial proton leak and efficiency, respectively, may make it difficult to reach definitive conclusions based solely on these measures.

A more direct approach to estimate coupling efficiency is to measure the P/O ratio (the amount of ADP consumed per mole of oxygen consumed; Gnaiger et al., 2000). P/O ratios provide a more informative measure of mitochondrial efficiency compared with RCRs as oxygen consumption is not necessarily directly proportional to ATP production because of the role of proton leak (Salin et al., 2015; Brand, 2005). P/O ratios have been shown to either decrease with increasing acclimation temperatures (Lannig et al., 2005) or be unaffected or minimally affected by thermal acclimation (Guderley and Johnston, 1996; Strobel et al., 2013; van den Thillart and Modderkolk, 1978). Similarly, direct assessment of proton leak can also be made by measuring proton leak kinetics, in which membrane potential ($\Delta\Psi_m$) and respiratory rates are measured under non-ADP-phosphorylating (leak) conditions following a titrated inhibition of the electron transport system (ETS). By comparing the resulting curves, proton leak can be compared at a common membrane potential (Divakaruni and Brand, 2011), which ensures that leak is measured at the same level of proton-motive force (PMF). Few studies have examined changes in mitochondrial proton leak kinetics with thermal acclimation. However, the available studies have found that proton leak decreases with cold acclimation (Jastroch et al., 2007; Trzcionka et al., 2008).

Department of Zoology, University of British Columbia, 6270 University Blvd., Vancouver, British Columbia, Canada V6T 1Z4.

*Author for correspondence (hbryant@zoology.ubc.ca)

 H.J.B., 0000-0002-8553-7792; D.J.C., 0000-0002-0329-3828; P.M.S., 0000-0002-5237-8836

Received 8 June 2018; Accepted 18 October 2018

List of symbols and abbreviations

ADP	adenosine diphosphate
ANT	adenine nucleotide translocase
ATP	adenosine triphosphate
BAT	brown adipose tissue
BSA	bovine serum albumin
Cat	carboxyatractylolide
C_q	mean cycle number
ETS	electron transport system
FCCP	carbonyl cyanide <i>p</i> -(trifluoromethoxy)phenyl-hydrazone
FDR	false discovery rate
GDP	guanosine-5'-diphosphate
GTP	guanosine-5'-triphosphate
IMM	inner mitochondrial membrane
PMF	proton-motive force
P/O	ratio of moles of ADP consumed per mole of oxygen
RCR	respiratory control ratio
ROS	reactive oxygen species
TPP ⁺	tetraphenylphosphonium ion
UCP	uncoupling protein
$\Delta\Psi_m$	membrane potential

Mitochondrial proton leak contributes to approximately 20% of standard metabolic rate in both endothermic and ectothermic vertebrates (Brand et al., 1991, 1994; Porter and Brand, 1993; Rolfe et al., 1999; Bishop and Brand, 2000). Although the mechanisms of this leak are not fully understood, it is thought to occur through a variety of pathways including protons moving directly across the membrane (although this contribution is small) or through proteins such as the adenine nucleotide translocase (ANT) and uncoupling proteins (UCPs) (Jastroch et al., 2010; Divakaruni and Brand, 2011). There is some evidence that UCPs may be differentially regulated in response to thermal acclimation in ectotherms and thus play a role in the modulation of mitochondrial function with temperature (Jastroch et al., 2005, 2007; Murakami et al., 2015; Wen et al., 2015; Tseng et al., 2011; dos Santos et al., 2013b; Mark et al., 2006). The function of UCPs is best understood in mammalian brown adipose tissue (BAT), where UCP1 acts to decrease the PMF, resulting in futile energy cycling and thermogenesis (Nicholls, 2001). But there are other isoforms of UCPs, including other members of the core UCP family (UCP2 and UCP3) and more distantly related UCPs (UCP4 and UCP5) (Esteves and Brand, 2005; Rousset et al., 2004). These isoforms have been proposed to play a role in attenuating reactive oxygen species (ROS) production, transporting fatty acids, and perhaps ROS signaling and insulin secretion (for a review, see Brand and Esteves, 2005). UCP isoforms have been identified in a variety of species and taxa, including plants and ectothermic organisms, but the functional roles of UCPs in non-endothermic taxa are still unclear (Woyda-Ploszczyca and Jarmuszkiwicz, 2017).

Here, we used Atlantic killifish, *Fundulus heteroclitus* (Linnaeus 1766), to investigate the influence of thermal acclimation and putative local adaptation on mitochondrial $\Delta\Psi_m$, proton leak and P/O ratios. We also explored the role of changes in UCPs in these processes by examining *Ucp* mRNA expression and the effects of palmitate, a known activator of mammalian UCP, on proton leak. Atlantic killifish are extremely eurythermal, and northern and southern populations of this species experience different local thermal conditions (Schulte, 2007). For example, mean monthly temperatures in Georgia, USA, exceed 25°C from June through September, and frequently reach this level in May, whereas temperatures seldom reach this level even in midsummer in

New Hampshire, USA (NOAA, National Estuarine Research Reserve System 2013–2017 station codes GRBLR and SAPLD; <http://www.nerrsdata.org/>). In contrast, in the winter, New Hampshire marshes are ice covered, whereas mean monthly winter temperatures in Georgia remain above 10°C. Consistent with these differences in environmental temperatures, northern and southern killifish have been shown to exhibit intraspecific variation in their thermal preferences, thermal tolerances and responses to thermal acclimation, suggestive of local adaptation (Chung and Schulte, 2015; Chung et al., 2017; Fangué et al., 2006, 2009a,b; Healy and Schulte, 2012; Healy et al., 2017; McBryan et al., 2016). The mitochondrial properties of *F. heteroclitus* have been previously shown to respond to thermal acclimation and differ between the northern and southern subspecies (Chung et al., 2017, 2018; Fangué et al., 2009b), making this an ideal model in which to investigate the role of changes in proton leak in thermal acclimation and adaptation. Northern killifish have been shown to have a greater liver mitochondrial maximal O₂ consumption rate than southern killifish following cold acclimation, and this increase in capacity in the northern subspecies following cold acclimation may be consistent with cold compensation of mitochondrial function (Chung and Schulte, 2015; Fangué et al., 2009b). Furthermore, ROS production in northern killifish has been shown to be influenced by acute changes in temperature, but not thermal acclimation (Chung and Schulte, 2015), suggesting that killifish may have mechanisms, such as UCPs, that respond to thermal acclimation in order to mitigate changes in the PMF and ROS production.

We hypothesized that adjustments to $\Delta\Psi_m$ and proton leak are involved in thermal adaptation and acclimation and therefore predicted that *Ucp* mRNA expression and fatty-acid-induced uncoupling would differ between subspecies and in response to thermal acclimation. The specific objectives of this study were to: (1) characterize the mRNA expression patterns of *Ucp* isoforms across tissues and determine how these patterns differ between subspecies following acclimation to high and low temperatures; (2) determine the effects of both warm and cold acclimation on mitochondrial respiratory capacity, P/O ratios, $\Delta\Psi_m$ and fatty-acid-induced uncoupling in killifish liver mitochondria; and (3) determine whether changes in *Ucp* mRNA expression in the liver correspond to changes in fatty-acid-induced uncoupling. This work demonstrates that $\Delta\Psi_m$ and proton leak are altered in response to thermal acclimation and these responses differ between subspecies that are putatively adapted to different thermal environments, and supports a role for UCPs as a potential mechanism for mitigating thermally induced changes to the PMF.

MATERIALS AND METHODS**Identification of *Ucp* isoforms**

Nucleotide BLAST was used to identify gene sequences in the *F. heteroclitus* genome (*Fundulus_heteroclitus*-3.0.2, GCF_000826765.1, annotation release 101) that share significant sequence similarity with *Ucp1*, *Ucp2*, *Ucp3*, *Ucp3L* and *Ucp5* as characterized in other tetrapod and fish species (no sequence similar to *Ucp4* was detected). Gene sequences for the *Ucp* isoforms from an additional five fish species and eight tetrapod species were also gathered from the NCBI and Ensembl databases (see Table 1 for accession numbers). MUSCLE alignment (Edgar, 2004) and phylogenetic analysis were performed using MEGA (v. 6.06, <https://www.megasoftware.net/>) to identify which of the *F. heteroclitus* *Ucp* isoforms were homologous with each of the *Ucp* family members identified in other species. A maximum likelihood (ML) tree (substitution type: nucleotide; model/method: Tamura–

Table 1. Accession numbers for gene sequences used in phylogenetic analyses

Group	Species	<i>Ucp1</i> gene ID	<i>Ucp2</i> gene ID	<i>Ucp3</i> gene ID	<i>Ucp3L</i> gene ID	<i>Ucp5</i> gene ID	
Tetrapods	<i>Anolis carolinensis</i>		ENSACAG00000006491 XM_008124024.2	ENSACAG00000009396 XM_003229550.2			
	<i>Gallus gallus</i>			ENSGALG00000017316 XM_015280964.1			
	<i>Bos taurus</i>	ENSBTAG00000004647 NM_001166528.1	ENSBTAG00000003692 NM_001033611.2	ENSBTAG00000005259 NM_174210.1		ENSBTAG00000016263 NM_001046145.1	
	<i>Loxodonta africana</i>	ENSLAFG00000007077 XM_010590606.1	ENSLAFG00000015866 XM_003420045.2	ENSLAFG00000005399 XM_003420044.2		ENSLAFG00000002284 XM_010594644.1	
	<i>Homo sapiens</i>	ENSG00000109424 NM_021833.4	ENSG00000175567 NM_003355.2	ENSG00000175564 NM_003356.3		ENSG00000102078 NM_001282195.1	
	<i>Mus musculus</i>	ENSMUSG00000031710 NM_009463.3	ENSMUSG00000033685 NM_011671.5	ENSMUSG00000032942 NM_009464.3		ENSMUSG00000031105 NM_011398.3	
	<i>Rattus norvegicus</i>	ENSRNOG00000003580 NM_012682.2	ENSRNOG00000017854 NM_019354.3	ENSRNOG00000017716 NM_013167.2		ENSRNOG00000006871 NM_053501.2	
	<i>Xenopus tropicalis</i>	ENSXETG00000014927 NM_001113882.1	ENSXETG00000026447 NM_203848.1				
	Fish	<i>Fundulus heteroclitus</i>	XM_012862869.1	XM_012867200.1	XM_012867201.1	XM_012851672.1	XM_012868877.1
		<i>Oryzias latipes</i>	ENSORLG00000018506	ENSORLG00000009082 ENSORLT00000011391.1	ENSORLG00000009082 ENSORLT00000011397.1	ENSORLG00000004325	ENSORLG00000015482
<i>Gasterosteus aculeatus</i>		ENSGACG00000017283	ENSGACG00000020354*	ENSGACG00000020354*	ENSGACG00000011266	ENSGACG00000020832	
<i>Takifugu rubripes</i>		ENSTRUG00000013144	ENSTRUG00000014496	ENSTRUG00000006965	ENSTRUG00000014470	ENSTRUG00000009205	
<i>Tetraodon nigriviridis</i>		ENSTNIG00000006838	ENSTNIG00000011803	ENSTNIG00000016239	ENSTNIG00000011804	ENSTNIG00000007592	
<i>Danio rerio</i>		ENSDARG00000023151	ENSDARG00000043154	ENSDARG00000091209		ENSDARG00000026680	

**Ucp2* and *Ucp3* in the *G. aculeatus* genome are labeled as the same gene and transcript. *Ucp2* and *Ucp3* are known to be adjacent to each other in animal genomes (Tine et al., 2012). However, phylogenetic analysis indicates they are separate *Ucp2* and *Ucp3* genes.

Nei model; rates among sites: uniform rates; gaps/missing data treatment: complete deletion; all codon positions selected; ML heuristic method: nearest-neighbor interchange) was constructed, and the reliability of the tree was confirmed by bootstrapping with 1500 replicates.

As an additional method to confirm the identification of homologous relationships, the genes adjacent to the various *Ucp* isoforms were identified in multiple species using Genomicus (v. 89.02, <http://www.genomicus.biologie.ens.fr/genomicus-89.02>) with all Ensembl vertebrate genomes. The genes surrounding each *Ucp* were also identified in the *F. heteroclitus* genome, and these gene lists were compared with those identified in other species using Genomicus to confirm syntenic relationships.

Animals and temperature acclimations for mRNA expression

All procedures and animal care were performed in accordance with the Canadian Council on Animal Care (CCAC) approved animal use protocol A11-0732. For mRNA expression data, adult southern killifish (*Fundulus heteroclitus heteroclitus*) were collected from Jekyll Island, GA, USA (31°02'N, 81°25'W; 69% male), and adult northern killifish (*Fundulus heteroclitus macrolepidotus*) were wild-caught by Aquatic Research Organisms (Hampton, NH, USA) from Taylor River, NH, USA (42°55'N, 70°51'W; 31% male), in the summer of 2014 and brought to holding facilities at The University of British Columbia in Vancouver, British Columbia, Canada. Based on their sizes, all animals were approximately 3–4 years of age (Kneib and Stiven, 1978). All *F. heteroclitus* were then held under common conditions of 15°C (a temperature experienced by both populations in the wild; Schulte, 2007), 20 ppt salinity and a 12 h:12 h light:dark photoperiod in 190 liter recirculating fiberglass tanks with biological filtration. All fish were fed daily to satiation throughout holding and acclimations with Nutrafin Max[®] flake food (Hagen, Inc., Baie d'Urfé, QC, Canada). After at least 4 weeks under these conditions, fish were transferred to experimental tanks at a density of approximately 1 fish per 6 liters. Different subspecies remained in separate tanks. Fish were then held in the experimental tanks under the conditions described above for at least 3 weeks before temperature acclimations began.

Temperature acclimations occurred at four different temperatures (5, 15, 25 and 33°C) with one tank for each subspecies acclimated to each temperature. These acclimation temperatures were chosen such that southern fish would be exposed to low temperatures that they would rarely experience in nature, and northern fish would be exposed to high temperatures that they would rarely experience in nature. For example, water temperature data from the coast of New Hampshire (station GRBLR, NOAA, NERRS January 2013–December 2017) recorded an average of only 25.6 days per year at 25°C or above, and mean monthly temperatures seldom reach this level. In contrast, data from the coast of Georgia (station SAPLD, NOAA, NERRS 2013–2017) indicate that fish experience an average of 143 days per year at 25°C or above, with mean monthly temperatures at this level or above throughout the summer. Note that even in Georgia, mean monthly temperatures never reach 33°C, only approaching this temperature on individual days. Similarly, at the low end of the temperature range, water data from the coast of Georgia only include four days at or below 5°C since 2013 (station SAPLD, NOAA, NERRS January 2013–June 2018), whereas water temperatures off the coast of New Hampshire are not measured from mid-December to mid-April, because the loggers are removed owing to the presence of ice (station GRBLR, NOAA, NERRS January 2013–June 2018). Tanks were brought to acclimation temperatures at a rate of change of approximately 2–3°C h⁻¹ and were then held at that temperature for 3 weeks. Following the acclimation period, fish were fasted for 24 h and then euthanized via cervical dislocation, and then sex, mass and length were assessed. Whole-animal data are presented in Fig. S1. Whole brain, whole gill basket, liver and a lateral skeletal muscle sample ventral to the dorsal fin were dissected and flash-frozen in liquid nitrogen. The whole process from the fish being removed to all tissues being flash-frozen took less than 5 min.

RNA isolations and cDNA synthesis

Tissues were homogenized in TRIzol[®] Reagent using a Bullet Blender[™] 24 (Next Advance, Inc., Averill Park, NY, USA) and isolated following the manufacturer's instructions (Life Technologies, Grand Island, NY, USA). Isolated RNA was then

checked for genomic contamination by running qRT-PCRs with 16 randomly selected non-reverse transcribed samples per tissue using the primers for the most highly expressed isoform in each respective tissue. If genomic contamination was present at a ratio greater than 1:16,000, RNA was put through a Qiagen on-column RNA clean-up using a Qiagen RNeasy Mini Kit and Qiagen RNase-free DNase. A total of 2 µg of RNA for liver and gill tissue and 1 µg of RNA for brain and muscle tissue was reverse transcribed into cDNA in a total volume of 20 µl using a High-Capacity cDNA Reverse Transcription Kit with random hexamers according to the manufacturer's instructions (Life Technologies). cDNA for each tissue was diluted 5-fold and a five-point standard curve was made for each tissue from pooling all samples per tissue. For 18S rRNA expression, cDNA was diluted 300-fold.

Quantitative real-time PCR (qRT-PCR)

qRT-PCR was performed on Bio-Rad CFX96 Touch™ Real-Time PCR Detection System (Bio-Rad Laboratories, Inc., Mississauga, ON, Canada). The qRT-PCR reaction protocol was as follows: 10 min at 95°C, and then 40 cycles of: 15 s at 95°C, 1 min at 60°C. A melt curve analysis from 65 to 95°C at an increment of 0.5°C was then conducted to ensure the presence of only one amplicon. Reactions of 20 µl total volume contained 5 µl of diluted cDNA, 0.4 µl of each primer, 10 µl of SYBR green master mix and 4.2 µl water. See Table 2 for qRT-PCR primer sequences. Primer pairs were designed using Primer Express (v. 3.0; ThermoFisher Scientific) in regions that were different between isoforms, but the same between any transcript variants. Specificity was confirmed via BLAST against the *F. heteroclitus* genome in GenBank. Thresholds across primer pairs within a tissue were set to the same value and gene expression levels were calculated as per Eqn 1:

$$\text{exp.} = (10^{(-1/\text{slope})})^{-C_q} \quad (1)$$

The slope was calculated from the standard curve, and C_q represents the mean cycle number for each sample (run in duplicate, $\sigma < 20\%$). No-template controls showed no signal across all plates, and other plate quality control parameters can be found in Table 2. All absolute gene expression values are normalized to 18S rRNA expression, calculated as described above.

Animals and temperature acclimations for isolated mitochondria

All procedures and animal care were performed in accordance with the Canadian Council on Animal Care approved animal use protocol A16-0028. Adult northern Atlantic killifish (*F. h. macrolepidotus*, 56% male) were wild-caught by Aquatic Research Organisms from

Taylor River, NH, USA (42°55'N, 70°51'W), and adult southern Atlantic killifish (*F. h. heteroclitus*, 44% male) were wild-caught from Jekyll Island, GA, USA (31°02'N, 81°25'W) in the autumn of 2016. Fish were then brought back to and housed at The University of British Columbia in 114 liter glass tanks at 15°C, 20 ppt salinity and a 12 h:12 h light:dark photoperiod for at least 4 months prior to acclimation. Fish were fed once daily to satiation with Nutrafin Max® flake food. Following this holding period, fish were acclimated in the same tanks to 5, 15 or 25°C with no other change in water parameters or photoperiod. These temperatures were chosen for the reasons described above, but the 33°C acclimation was omitted because this is not environmentally relevant for either population. Tanks were brought to the acclimation temperatures at a rate of change of approximately 2–3°C h⁻¹ and then held at the acclimation temperature for 3 weeks prior to sampling.

Mitochondrial isolations

Chemicals for mitochondrial isolations were obtained from Sigma-Aldrich (St Louis, MO, USA) with the exception of bovine serum albumin (BSA), which was obtained from Akron Biotech (Boca Raton, FL, USA). Livers from seven fish were pooled for each mitochondrial sample. Prior to euthanasia, fish sex, mass and length were recorded (Fig. S2). Fish were then euthanized via rapid cervical dislocation and liver tissue was taken. Livers were weighed and then placed in ice-cold homogenization buffer (250 mmol l⁻¹ sucrose, 50 mmol l⁻¹ KCl, 0.5 mmol l⁻¹ EGTA, 25 mmol l⁻¹ KH₂PO₄, 10 mmol l⁻¹ Hepes, 1.5% w/v BSA, pH 7.4 at 20°C). Liver tissue was minced in the ice-cold homogenization buffer until pieces were approximately 1 mm³ in size and then homogenized using seven passes of a loose-fitting Teflon pestle. This crude homogenate was filtered through one-ply cheesecloth and centrifuged at 600 g for 10 min at 4°C. The fat layer was aspirated from the supernatant and the supernatant was filtered through four-ply cheesecloth. The defatted supernatant was centrifuged at 6000 g for 10 min at 4°C and the resulting pellet was washed two times with fresh ice-cold homogenization buffer at 6000 g for 10 min at 4°C. Any remaining homogenization buffer was aspirated from the pellet and the pellet was suspended in 300 µl BSA-free ice-cold homogenization buffer. Liver mitochondria suspensions were kept on ice until respiration and $\Delta\Psi_m$ measurements were completed, which was within 6 h of mitochondrial isolation. Protein concentrations in each sample were determined prior to measurements using a Bradford (1976) assay with BSA standards.

Table 2. Primer pairs and plate parameters for qRT-PCR

Gene	Primer	Sequence (5'–3')	Efficiency			Melt temperature (°C)
			(%)	Slope	Y-intercept	
<i>Ucp1</i>	F	GCT TCG TCA CCA CCG TCA T	97.0	–3.397	16.323	0.997
	R	GGA GAG TTC ATG TAT CTG GTC TTC AC				
<i>Ucp2</i>	F	CCT GCC TTG CCA CTT CGT	91.9	–3.535	28.644	0.995
	R	AAG CGA TCA CAG TCG TGC ATA				
<i>Ucp3</i>	F	GGC GAG GCT CAC AAC GTT	92.3	–3.521	22.272	0.998
	R	CGA ACA CGC CCC GAT ACT				
<i>Ucp3-like</i>	F	CAG GTT CCA GGC TCA GAT ACG	91	–3.559	24.513	0.996
	R	TGC CGC TGT ACC TCT TCA CA				
<i>Ucp5</i>	F	GCC TCA TAC GGC ACA ATC AA	84.5	–3.760	23.262	0.999
	R	CGA CTG ACG AAC AGC CTC TTC				
18S (designed by Whitehead et al., 2011)	F	TTC CGA TTA ACG AAC GAG AC	98	–3.372	14.142	0.998
	R	GAC ATC TAA GGG CAT CAC AG				

Mitochondrial respiration and membrane potential measurements

Chemicals for mitochondrial respiration and membrane potential measurements were obtained from Sigma-Aldrich except for carboxyatractyloside (Cat), which was obtained from EMD Millipore (Etobicoke, ON, Canada). All mitochondrial respiration and mitochondrial $\Delta\Psi_m$ measurements were determined via high-resolution respirometry using an Oxygraph O2k system and tetraphenylphosphonium (TPP⁺)-selective electrodes (Oroboros Instruments, Innsbruck, Austria) at an assay temperature of 15°C. O₂ electrodes were calibrated with air-saturated and O₂-depleted assay buffer (MiRO5, 110 mmol l⁻¹ sucrose, 0.5 mmol l⁻¹ EGTA, 3 mmol l⁻¹ MgCl₂, 60 mmol l⁻¹ K-lactobionate, 20 mmol l⁻¹ taurine, 10 mmol l⁻¹ KH₂PO₄, 20 mmol l⁻¹ Hepes, 0.1% w/v BSA, pH 7.1 at 30°C; Gnaiger and Kuznetsov, 2002) and were calibrated for background O₂ consumption at 15°C using published O₂ solubilities (Forstner and Gnaiger, 1983). All values measured by TPP⁺-selective electrodes were corrected for chemical background and dilution effects. $\Delta\Psi_m$ was calculated as described in Chung and Schulte (2015).

Liver mitochondrial protein (0.1–0.2 mg) was loaded into 2 ml MiRO5 followed by rotenone (0.5 $\mu\text{mol l}^{-1}$ dissolved in ethanol) to inhibit complex I and succinate (10 mmol l⁻¹, complex II substrate) to measure state II respiration, and then ADP (125 $\mu\text{mol l}^{-1}$) was added to measure state III respiration. The ADP was then allowed to be completely consumed to determine the P/O ratio. P/O ratios were calculated according to Gnaiger et al. (2000). Saturating ADP (1.25 mmol l⁻¹) was then added to reinitiate state III respiration and then oligomycin (2.5 $\mu\text{mol l}^{-1}$ dissolved in ethanol) was added to induce state IV respiration. Finally, carbonyl cyanide *p*-(trifluoromethoxy) phenyl-hydrazone (FCCP; 1 $\mu\text{mol l}^{-1}$ dissolved in ethanol) was added to achieve maximum electron transport flux by completely uncoupling the mitochondria. Only complex II respiration rates were measured in order to be consistent with the measurement of proton leak kinetics, where malonate is used to titrate inhibition through complex II (Affourtit et al., 2018). Furthermore, complex-I-mediated respiration rates have previously been measured in both northern and southern *F. heteroclitus* (Chung et al., 2017, 2018).

At the beginning of each proton leak kinetic curve assay, rotenone (0.5 $\mu\text{mol l}^{-1}$ dissolved in ethanol), oligomycin (2.5 $\mu\text{mol l}^{-1}$ dissolved in ethanol) and Cat (5 $\mu\text{mol l}^{-1}$) were added to the chamber containing 2 ml MiRO5. Nigericin was not included because it has an inhibitory effect on killifish liver mitochondrial respiration (Chung and Schulte, 2015). Cat was included to inhibit the activity of the ANT to specifically assess the potential role of UCPs in proton conductance. Preliminary data indicated the addition of the same volume of 50% ethanol did not influence $\Delta\Psi_m$ or respiration rates. TPP⁺-selective electrodes were introduced and calibrated through five additions of TPP⁺ (one 1 $\mu\text{mol l}^{-1}$ addition followed by four 0.5 $\mu\text{mol l}^{-1}$ additions for a total of 3 $\mu\text{mol l}^{-1}$ TPP⁺). Liver mitochondrial protein (0.7–0.8 mg) was then added, followed by succinate (10 mmol l⁻¹) to achieve state II respiration. State II respiration was then titrated using nine additions of malonate (0.5 mmol l⁻¹ each, for a total of 4.5 mmol l⁻¹) and then mitochondria were uncoupled through the addition of FCCP (1 $\mu\text{mol l}^{-1}$ dissolved in ethanol). Each proton leak kinetic curve was fit to a combined model equation (Eqn 2):

$$f(x) = ax + b \times \exp^{(cx)}, \quad (2)$$

where x is membrane potential (mV), using GraphPad Prism 7 software (La Jolla, CA, USA). This combined model accounts for

both the ohmic (linear) and non-ohmic (exponential) behavior that has been previously described for mitochondrial proton leak kinetics (Jastroch et al., 2012; Murphy, 1989; Nicholls, 1977).

A separate set of assays was performed with the inclusion of palmitate to stimulate UCP activity. For these treatments only, sodium palmitate (35 $\mu\text{mol l}^{-1}$ dissolved in 50% ethanol) was added at the beginning of each run. This results in approximately 11.8 nmol l⁻¹ free palmitate in the respiration medium (Richieri et al., 1993). Guanosine-5'-triphosphate (GTP) and guanosine-5'-diphosphate (GDP; known inhibitors of mammalian UCP1) were also tested at multiple concentrations (see Results for details).

Statistical analysis

All statistical analyses were conducted in R (v3.3.2; <https://www.r-project.org/>). All data are presented as means \pm s.e.m. and α was set to 0.05. Assumptions of normality of residuals and homogeneity of variances were assessed using a Shapiro–Wilk test and a Bartlett test, respectively. Data were log transformed where necessary to meet parametric assumptions. For tissue-specific expression of *Ucp* isoform mRNAs, one-way ANOVAs followed by Tukey honest significant difference tests were used where parametric assumptions were met. Where parametric assumptions were not met, we utilized Kruskal–Wallis rank sum tests followed by Mann–Whitney *U*/Wilcoxon rank sum tests. For assessing changes in gene expression and mitochondrial respiration measurements across acclimation temperatures and between subspecies comparisons, we utilized two-way ANOVAs. Where parametric assumptions were met, *post hoc* analyses were performed using planned comparison *t*-tests followed by false discovery rate (FDR) correction. In cases where parametric assumptions were not met, *post hoc* analyses were completed via pair-wise comparisons using a Mann–Whitney *U*/Wilcoxon rank sum test with FDR-corrected *P*-values. All mRNA expression values in figures have been multiplied by a factor of 10⁵ for ease of visual presentation. RCRs were calculated as state III/state IV (Chance and Williams, 1955; Gnaiger, 2014). Identifying acclimation and subspecies effects on proton leak kinetic was achieved by comparing leak respiration at the highest common $\Delta\Psi_m$ (150.6 mV) among proton leak kinetic curves. Comparisons of the effect of thermal acclimation on the palmitate response were achieved using *t*-tests comparing oxygen consumption rate under control and palmitate-treated conditions at the $\Delta\Psi_m$ where the largest difference between the control and palmitate curves was present (northern: 5°C at 164 mV, 15°C at 165 mV and 25°C at 158 mV; southern: 5°C at 151 mV, 15°C at 142 mV and 25°C at 145 mV).

RESULTS

Phylogenetic and syntenic analyses

We identified five UCP homologues in *F. heteroclitus* using phylogenetic analysis (Fig. 1). The sequences for the different isoforms from fish were generally more similar to the same isoform from tetrapods than they were to the other fish isoforms. Therefore, the *F. heteroclitus* isoforms were given the name of their mammalian counterpart where possible. Syntenic analysis confirmed this naming, as the adjacent genes were generally conserved between fish and tetrapods. In the case of the apparent fish-specific *Ucp3L*, the isoform was named based on the naming convention in other fish species, and syntenic analysis also confirmed orthology within the fishes. We did not detect an isoform homologous to mammalian *Ucp4* in the *F. heteroclitus* genome. Note that the annotation of *Ucp* isoforms in the published fish genomes is poor. For example, some *Ucp* isoforms in fish

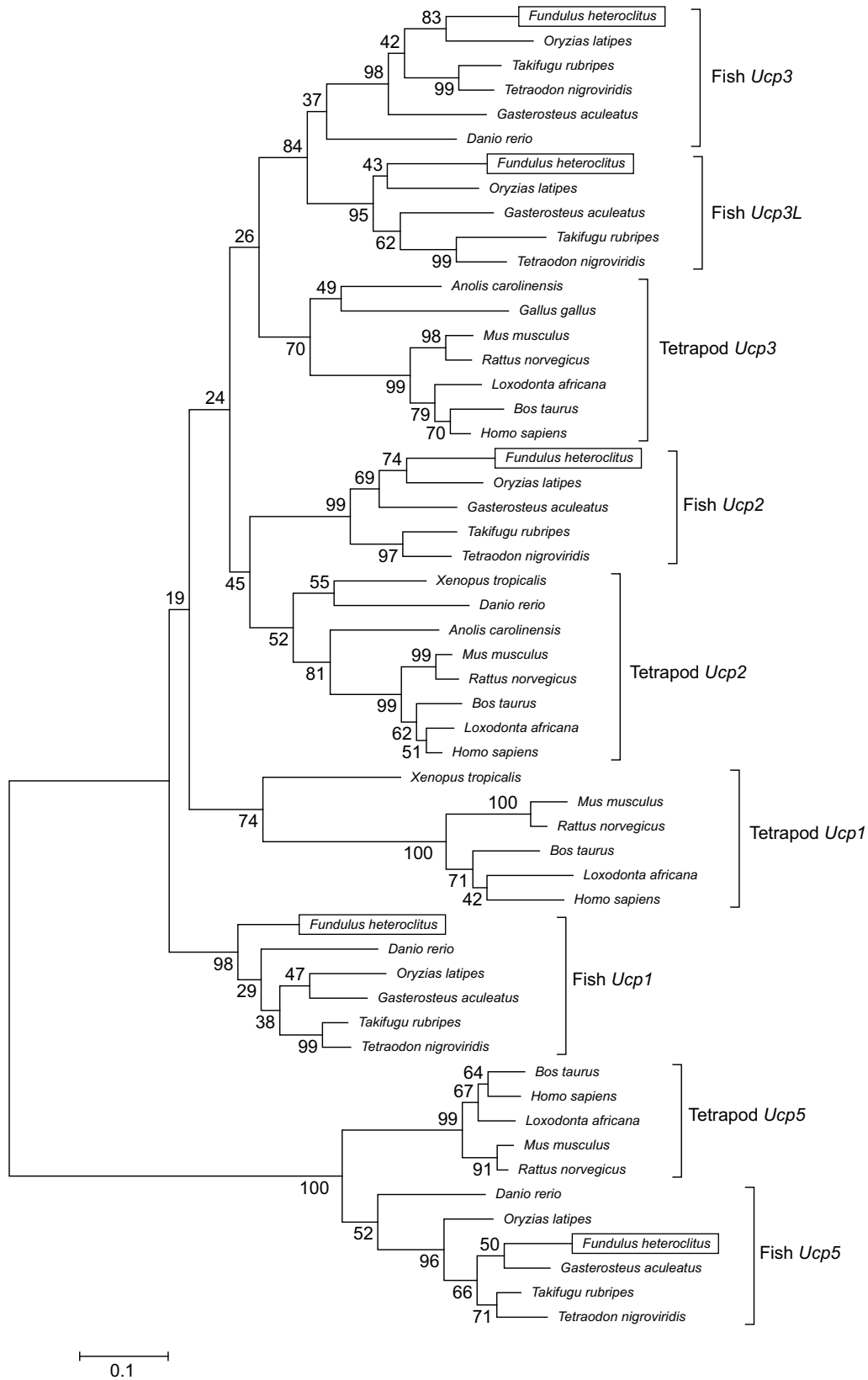


Fig. 1. Phylogenetic relationships among selected teleost and tetrapod *Ucp* gene sequences. This tree was constructed using maximum likelihood analysis of nucleotide sequences, rooted to the *Ucp5* gene sequences. Bootstrap values (from 1500 replicates) are shown at the nodes. Gene IDs for all sequences are listed in Table 1.

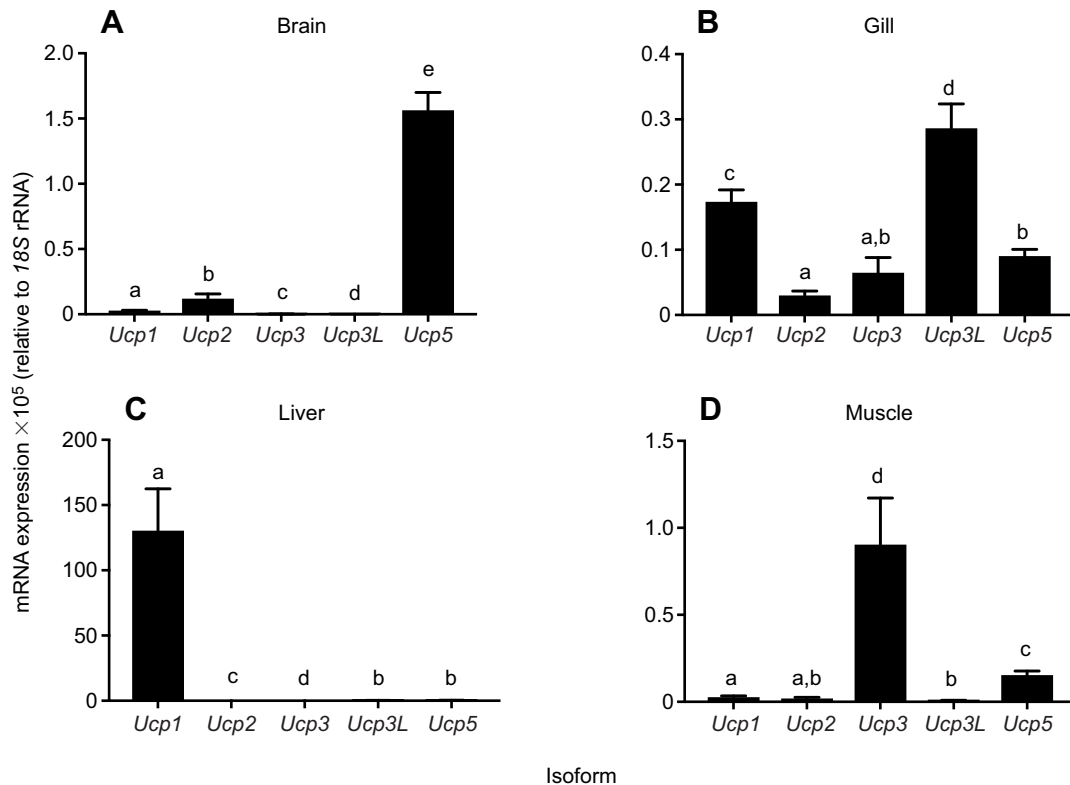


Fig. 2. mRNA expression of *Ucp* isoforms in tissue from northern *Fundulus heteroclitus* acclimated to 15°C. (A) Brain, (B) gill, (C) liver and (D) muscle. Data are means±s.e.m. expressed relative to 18S rRNA and multiplied by 10⁵ for clarity ($n=9$ for all groups). Different letters indicate a significant difference among isoforms within a tissue using Mann–Whitney *U* rank sum tests for A, B and D and a Tukey honest significant difference test for C.

genomes (both in Ensembl and GenBank) were labeled similarly to each other or as unknown proteins. In these cases, the genes were given the names of their mammalian counterparts based on the phylogenetic and syntenic relationships identified here.

Tissue-specific mRNA expression

The expression profiles of the five *Ucp* isoforms investigated here differed among tissues. In brain, there was high expression of *Ucp5* mRNA relative to the other isoforms ($P_{\text{isoform}} < 0.001$; Fig. 2A). In gill tissue, the fish-specific isoform *Ucp3L* was the most highly expressed, with *Ucp1* and *Ucp5* mRNAs being expressed at an intermediate level ($P_{\text{isoform}} < 0.001$; Fig. 2B). In liver tissue, *Ucp1* was the most highly expressed isoform ($P_{\text{isoform}} < 0.001$; Fig. 2C). In muscle, *Ucp3* was the most highly expressed isoform ($P_{\text{isoform}} < 0.001$; Fig. 2D).

Thermal acclimation and subspecies effects on *Ucp* isoform mRNA expression

The expression of *Ucp1*, the most highly expressed *Ucp* isoform in *F. heteroclitus* liver tissue, was significantly affected by acclimation ($P_{\text{acclimation}} < 0.001$; Fig. 3A) such that expression was lowest following acclimation to 25°C in both subspecies. *Ucp1* mRNA expression in the liver was higher in the northern subspecies than in the southern subspecies ($P_{\text{subspecies}} < 0.001$; Fig. 3A). There was an interaction between acclimation temperature and subspecies such that *Ucp1* decreased in mRNA expression following acclimation to 5°C in southern killifish, but not northern killifish, and the subspecies differed in *Ucp1* mRNA expression following acclimation to all temperatures except 15°C ($P_{\text{acclimation} \times \text{subspecies}} < 0.001$; Fig. 3A).

Similar to *Ucp1* in the liver, *Ucp5* in the brain ($P_{\text{subspecies}} < 0.001$; Fig. 3B) and *Ucp1* ($P_{\text{subspecies}} < 0.001$; Fig. 3D) and *Ucp5* ($P_{\text{subspecies}} < 0.001$; Fig. 3F) in the gill were expressed at higher levels in northern killifish than in southern killifish. Contrastingly, *Ucp3L* in gill tissue showed no difference between subspecies ($P_{\text{subspecies}} = 0.494$; Fig. 3E) and *Ucp3* in muscle tissue was generally expressed more highly in southern killifish than in northern killifish ($P_{\text{subspecies}} < 0.001$; Fig. 3C).

The most highly expressed isoforms in each tissue displayed different patterns of expression with thermal acclimation. *Ucp5* in both brain ($P_{\text{acclimation}} < 0.001$; Fig. 3B) and gill tissue ($P_{\text{acclimation}} < 0.001$, $P_{\text{acclimation} \times \text{subspecies}} = 0.265$; Fig. 3F) showed an increase in expression with decreasing acclimation temperature, although this was not seen in southern killifish brain tissue ($P_{\text{acclimation} \times \text{subspecies}} = 0.015$; Fig. 3B). Similarly, *Ucp3L* mRNA expression was higher following cold acclimation in the northern, but not southern, subspecies ($P_{\text{acclimation}} = 0.001$, $P_{\text{acclimation} \times \text{subspecies}} = 0.039$; Fig. 3E). In gill tissue, *Ucp1* mRNA expression increased with acclimation to extreme temperatures (5 and 33°C) ($P_{\text{acclimation}} = 0.014$, $P_{\text{acclimation} \times \text{subspecies}} = 0.704$; Fig. 3D). *Ucp3* in muscle tissue was affected by acclimation temperature ($P_{\text{acclimation}} = 0.005$; Fig. 3C), but this effect was only detected in northern killifish ($P_{\text{acclimation} \times \text{subspecies}} = 0.013$), which showed an increase in *Ucp3* mRNA expression following acclimation to 33°C.

Mitochondrial respiration

Liver mitochondrial state III respiration was greatest in 5°C-acclimated northern killifish when compared with 15°C- and 25°C-acclimated fish, and no thermal acclimation effects were observed in southern killifish ($P_{\text{acclimation}} = 0.025$,

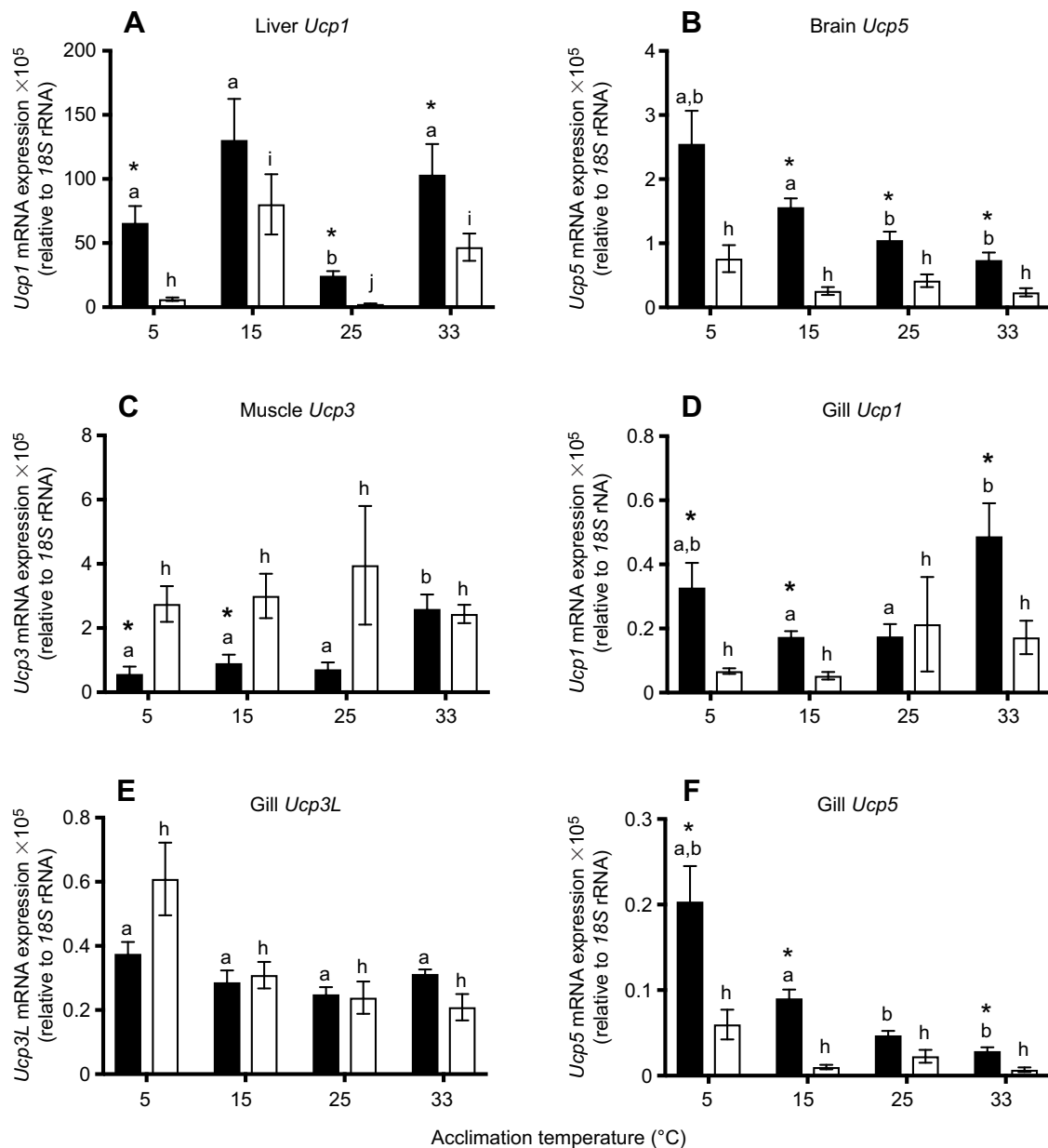


Fig. 3. mRNA of the most highly expressed *Ucp* isoforms within tissue from northern (black bars) and southern (white bars) *F. heteroclitus* acclimated to 5, 15, 25, and 33°C. (A) Liver (*Ucp1*), (B) brain (*Ucp5*), (C) muscle (*Ucp3*) and (D–F) gill (*Ucp1*, D; *Ucp3L*, E; *Ucp5*, F). Data are means±s.e.m. expressed relative to 18S rRNA expression and multiplied by 10⁵ for clarity ($n=7-9$ for each group). Different letters indicate a significant difference within a population and an asterisk indicates a significant difference between populations at a given acclimation temperature.

$P_{\text{acclimation} \times \text{subspecies}}=0.012$; Fig. 4A). Although there was no main effect of subspecies on state III respiration ($P_{\text{subspecies}}=0.055$), we detected greater mitochondrial respiration in northern *F. heteroclitus* following low temperature acclimation when compared with southern fish in *post hoc* analyses.

State IV (oligomycin) respiration in the liver did not differ significantly between northern and southern killifish, or with thermal acclimation ($P_{\text{acclimation}}=0.147$, $P_{\text{subspecies}}=0.067$; Fig. 4B). However, there was a significant interaction between these factors ($P_{\text{acclimation} \times \text{subspecies}}=0.032$) driven by a trend for state IV respiration to decrease with warm acclimation in northern killifish, but not southern, killifish, and for state IV respiration to decrease with cold acclimation in southern, but not northern, killifish (Fig. 4B).

RCRs in liver mitochondria, an estimate of mitochondrial coupling, were above 6 for both subspecies across acclimation temperatures, and were highest in northern killifish following acclimation to 5°C ($P_{\text{acclimation}}=0.011$, $P_{\text{subspecies}}=0.327$, $P_{\text{acclimation} \times \text{subspecies}}=0.258$; Fig. 4C).

FCCP-stimulated O₂ consumption rate differed between subspecies and with acclimation temperature, such that there was a large increase in FCCP-stimulated O₂ consumption rate in liver mitochondria from northern killifish, but not southern killifish, following acclimation to 5°C ($P_{\text{acclimation}}=0.006$, $P_{\text{subspecies}}=0.040$, $P_{\text{acclimation} \times \text{subspecies}}<0.001$; Fig. 4D).

P/O ratios differed between subspecies and with thermal acclimation ($P_{\text{acclimation}}<0.001$, $P_{\text{subspecies}}=0.015$; Fig. 5), although there was also a significant interaction between these two factors

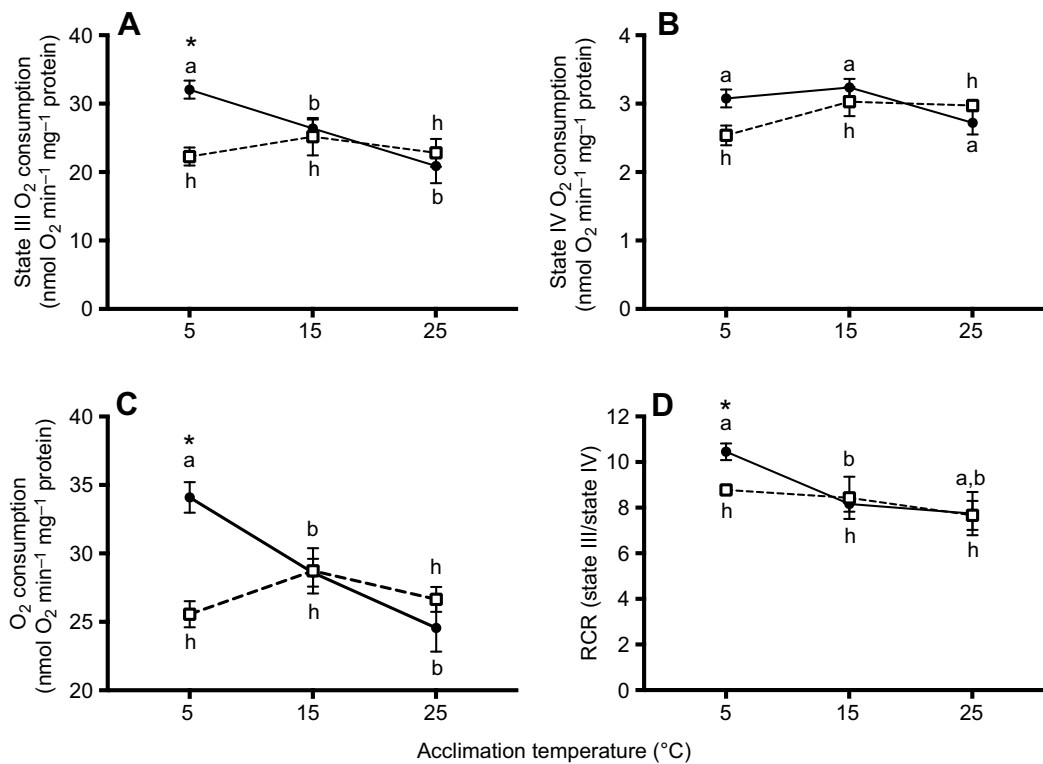


Fig. 4. Mitochondrial O₂ consumption rates (nmol O₂ min⁻¹ mg protein⁻¹) and respiratory control ratios (RCRs) for liver mitochondria from northern (black circles, solid line) and southern (white squares, dashed line) *F. heteroclitus* acclimated to 5, 15 and 25°C and assayed at 15°C. Data are means±s.e.m. ($n=5-6$ for each group). (A) State III (maximal ADP phosphorylating) respiration, (B) state IV (oligomycin) respiration, (C) FCCP-stimulated respiration and (D) RCR, the ratio of state III/state IV respiration. Different letters indicate a significant difference between acclimation temperatures within a population, and an asterisk indicates a significant difference between populations at a given acclimation temperature. Data were analyzed using (A,B,D) planned comparison *t*-tests followed by FDR correction and (C) a Mann–Whitney *U* rank sum test followed by FDR correction.

($P_{\text{acclimation} \times \text{subspecies}}=0.022$). In northern killifish, P/O ratios increased with acclimation to 5°C, but there was no effect of thermal acclimation on P/O ratios in southern killifish. Following acclimation to 25°C, southern killifish had greater P/O ratios than northern killifish (Fig. 5).

Thermal acclimation and subspecies effects on mitochondrial membrane potential

We examined mitochondrial membrane potential under state II (non-ADP phosphorylating) conditions by constructing a proton

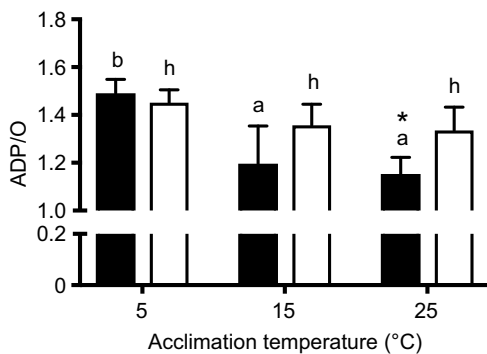


Fig. 5. P/O ratios for northern (black bars) and southern (white bars) *F. heteroclitus* acclimated to 5, 15 and 25°C and assayed at 15°C. Data are means±s.e.m. ($n=4-6$ for each group). Different letters indicate a significant difference within a population among acclimation temperatures as determined by planned comparison *t*-tests followed by FDR correction. An asterisk indicates a significant difference between populations at a given acclimation temperature.

leak kinetic curve through sequential inhibition of the ETS at complex II. The proton leak kinetic curves were strikingly different between northern and southern killifish (Fig. 6A,B). In northern killifish, there was a substantial impact of 5°C acclimation on the position of the curve, which was displaced to higher initial $\Delta\Psi_m$ and higher rates of oxygen consumption (Fig. 6A). This effect was not observed in mitochondria from southern killifish (Fig. 6B). In addition, mitochondria from northern killifish generally operated at higher $\Delta\Psi_m$ and with higher rates of oxygen consumption than mitochondria from southern killifish, and this difference was particularly evident in fish acclimated to 5°C (compare Fig. 6A,B). These effects were also evident when comparing the maximum (un-inhibited) state II $\Delta\Psi_m$ (Fig. 6C), as state II $\Delta\Psi_m$ was higher in northern killifish than in southern killifish ($P_{\text{subspecies}}<0.001$) at all acclimation temperatures. In northern killifish, state II $\Delta\Psi_m$ decreased with acclimation to increasing temperatures ($P_{\text{acclimation}}=0.016$), and this effect was not present in southern killifish ($P_{\text{acclimation} \times \text{subspecies}}=0.001$; Fig. 6C).

State II or state IV respiration is often used as a proxy for proton leak across the inner mitochondrial membrane, but accurate quantification of proton leak requires assessing leak-driven oxygen consumption at a defined value of the membrane potential, which can be derived from the proton leak kinetic curves. Quantification of changes in mitochondrial proton conductance (proton leak) across the inner mitochondrial membrane is usually performed by assessing O₂ consumption rate at the highest common $\Delta\Psi_m$ among treatments. When considering the average proton leak kinetic curves for each subspecies and all three acclimation treatments, the highest common $\Delta\Psi_m$ was 150.6 mV. At this membrane potential, northern

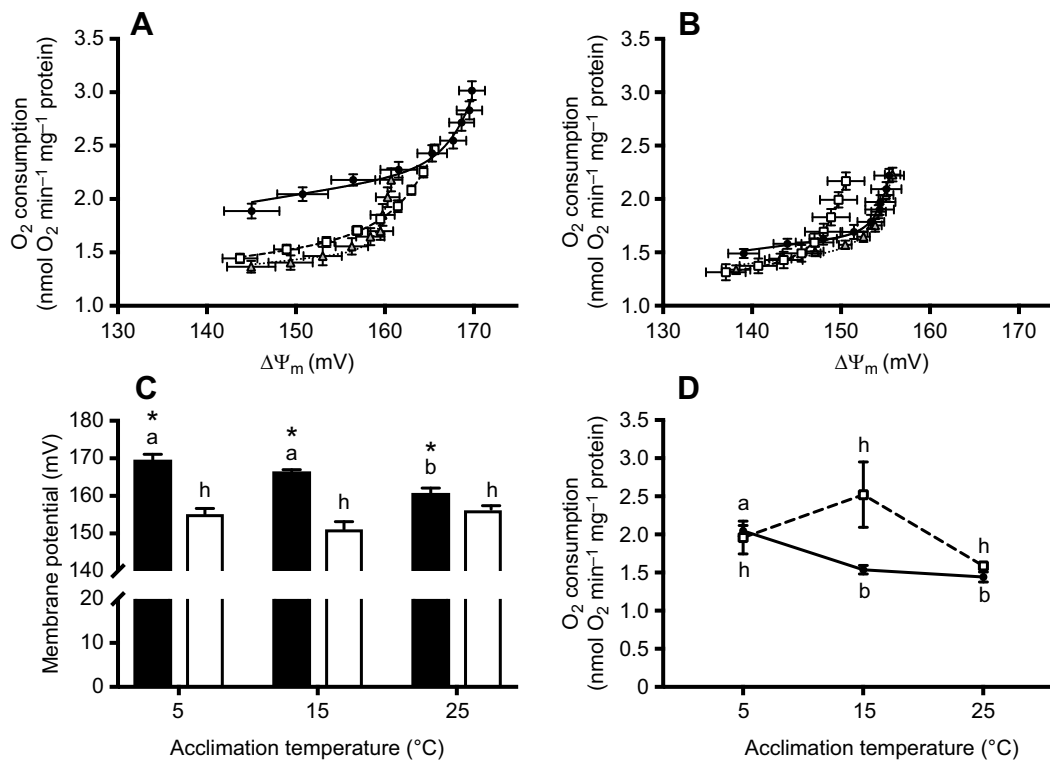


Fig. 6. Thermal acclimation and population effects on liver mitochondrial proton leak kinetics in *Fundulus heteroclitus*. (A) Proton leak kinetic curves from northern and (B) southern killifish acclimated to 5°C (black circles, solid line), 15°C (white squares, dashed line) and 25°C (gray triangles, dotted line). (C) State II membrane potential (mV) measured in liver mitochondria from northern (black bars) and southern (white bars) killifish acclimated to 5, 15 and 25°C. Data are means \pm s.e.m. ($n=6-7$ for all groups). (D) O₂ consumption rate (nmol O₂ min⁻¹ mg⁻¹ protein) at the highest common membrane potential ($\Delta\Psi_m$, 150.6 mV) from northern (black circles, solid line) and southern (white squares, dashed line) killifish acclimated to 5, 15 and 25°C and assayed at 15°C. Letters that differ indicate a significant difference within a population and an asterisk indicates significant differences between populations at a given acclimation temperature as determined by planned comparison *t*-tests followed by FDR corrections.

killifish liver mitochondria showed increased proton conductance following acclimation to 5°C, but southern killifish showed no difference in proton conductance with thermal acclimation ($P_{\text{acclimation} \times \text{subspecies}}=0.028$, $P_{\text{acclimation}}=0.010$; Fig. 6D). There was only a modest difference between the subspecies in proton conductance at the highest common membrane potential ($P_{\text{subspecies}}=0.041$), and this difference was not evident in *post hoc* analyses.

Taken together, these data suggest that there is little difference between the subspecies in the intrinsic proton conductance of the IMM (Fig. 6D), but that northern fish mitochondria tend to operate at a higher $\Delta\Psi_m$ with a resulting higher level of proton conductance (Fig. 6A–C), and that these differences are particularly evident when fish are acclimated to low temperatures.

Fatty-acid-induced uncoupling and thermal acclimation

UCP1, which is the dominant UCP isoform in killifish liver (Fig. 2), is known in mammals to be activated by free fatty acids of a variety of chain lengths, reactive alkenals and superoxide products, and to be inhibited by purine nucleotides (e.g. ADP, ATP, GDP and GTP) (Klingenberg and Huang, 1999; Davis et al., 2008; Shabalina et al., 2004). Here, we utilized palmitate, which is a known fatty-acid activator of UCPs, causing increases in mitochondrial O₂ consumption rate and decreases in $\Delta\Psi_m$ (e.g. Jastroch et al., 2007; dos Santos et al., 2013b; Jastroch et al., 2012), to assess the functional role of UCP1 in affecting proton conductance in killifish liver.

Preliminary analyses (data not shown) indicated that although killifish liver mitochondria responded to palmitate in the expected

manner (i.e. with a decrease in $\Delta\Psi_m$), the response could not be reversed by GDP or GTP. Several concentrations of GDP were tested and the effectiveness of the protocol used was assessed using mitochondria isolated from rat (*Rattus norvegicus*) BAT. In rat BAT mitochondria, the addition of palmitate caused a 29.4% increase in O₂ consumption rate and a 5% decrease in membrane potential. Upon administering GDP following the palmitate addition, O₂ consumption rate and membrane potential were restored by a 41.6% decrease and a 9.5% increase, respectively. In contrast, in killifish mitochondria, the increased respiration and decreased $\Delta\Psi_m$ that corresponded to the addition of palmitate was not inhibited by the addition of 8 mmol l⁻¹ glutamate (high extra-mitochondrial glutamate blocks the glutamate aspartate transporter; Samartsev et al., 1997), 6 μ mol l⁻¹ cyclosporine A (an inhibitor of the permeability transition pore) or 50 μ mol l⁻¹ genepin (a known inhibitor of UCP2) (data not shown). The addition of Cat (a known inhibitor of the adenine nucleotide translocator) resulted in the return of approximately 20% of the increase in respiration and decrease in $\Delta\Psi_m$ (data not shown), and thus 5 μ mol l⁻¹ Cat was included in every run to exclude the effects of the ANT on proton leak.

Exposure to palmitate caused a significant increase in O₂ consumption rate over control conditions in northern killifish liver mitochondria following acclimation to 5 and 15°C but not 25°C ($P_{5^\circ\text{C}}=0.038$, $P_{15^\circ\text{C}}=0.019$, $P_{25^\circ\text{C}}=0.296$; Figs 7A–C, 8A). In contrast, exposure to palmitate had no effect on O₂ consumption rate in southern killifish liver mitochondria at any acclimation temperature ($P_{5^\circ\text{C}}=0.937$, $P_{15^\circ\text{C}}=0.803$, $P_{25^\circ\text{C}}=0.396$; Figs 7D–F, 8B).

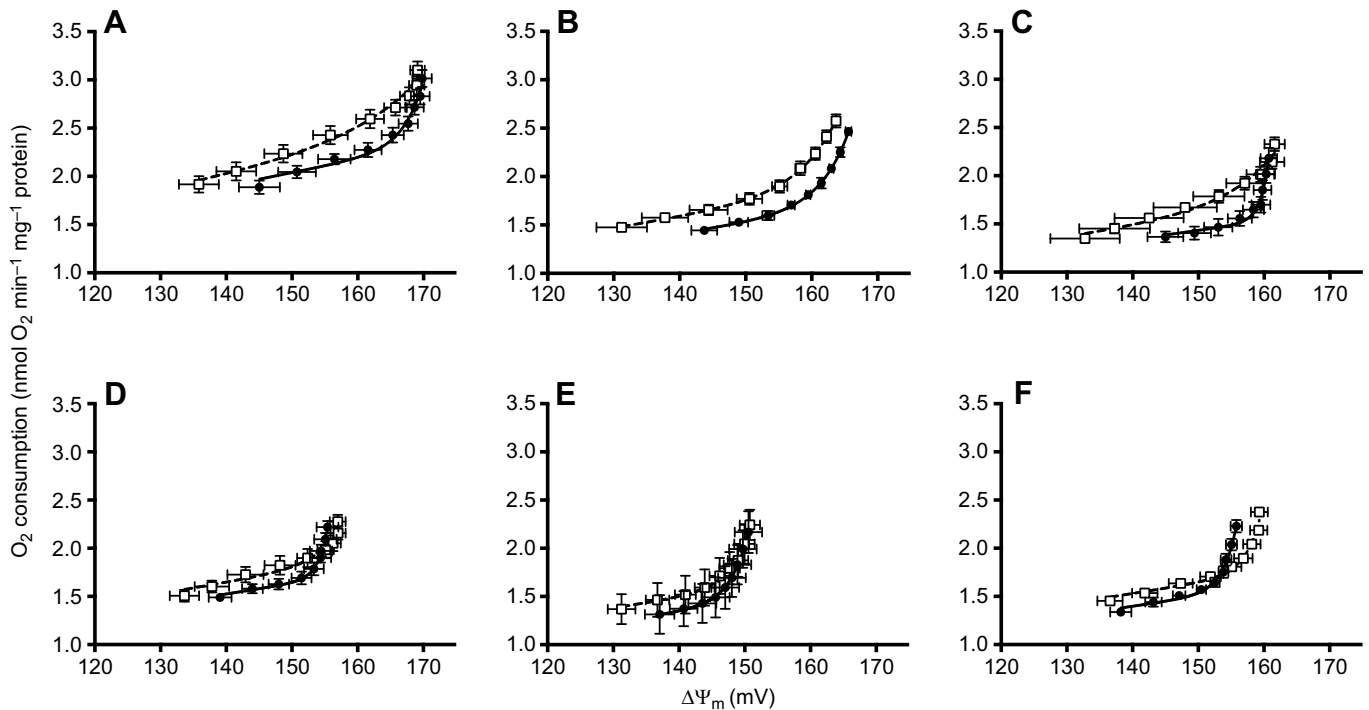


Fig. 7. Proton leak kinetic curves with or without palmitate for thermally acclimated northern and southern *Fundulus heteroclitus*. Proton leak kinetic curves for control (black circles, solid lines) and palmitate-treated ($35 \mu\text{mol l}^{-1}$, white squares, dashed lines) liver mitochondria from northern (A–C) and southern (D–F) *F. heteroclitus* acclimated to 5 (A,D), 15 (B,E) and 25°C (C,F) and assayed at 15°C. Data are means \pm s.e.m. ($n=6-7$ for all groups).

DISCUSSION

This study represents a comprehensive examination of the effects of thermal acclimation and adaptation on mitochondrial proton leak and efficiency in two subspecies of a eurythermal teleost, *F. heteroclitus*, and an examination of the potential role of UCPs in modulating these effects. The most striking pattern that we observed was a difference in the plasticity of proton leak and mitochondrial efficiency in response to temperature acclimation between northern and southern killifish. In liver mitochondria from northern killifish, cold acclimation caused an increase in both respiratory capacity and proton leak, and these effects were absent in southern killifish. But, paradoxically, this increase in proton leak was associated with an increase in P/O ratio in northern killifish at

low acclimation temperatures, suggesting that the increase in ATP-synthesizing capacity in northern killifish in response to cold was greater than the increase in proton leak. In liver, *Ucp1* was the primary UCP isoform expressed, and it was generally expressed at higher levels in northern killifish than in southern killifish. This is consistent with the observation that at a functional level, palmitate stimulation of proton leak was detectable only in mitochondria from northern killifish, suggesting there may be differences in UCP activity between subspecies. Taken together, these data indicate that northern killifish have an enhanced capacity to respond to cold acclimation relative to southern killifish, possibly associated with differences in the regulation and activity of UCPs.

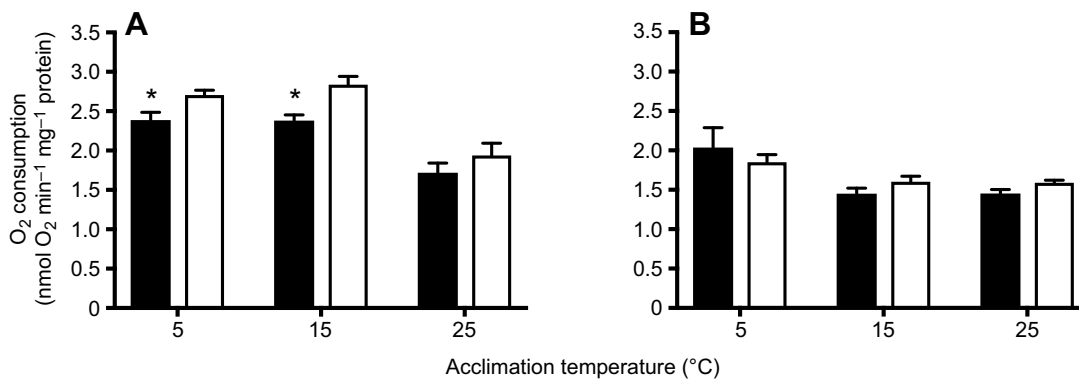


Fig. 8. State II O_2 consumption ($\text{nmol O}_2 \text{ min}^{-1} \text{ mg}^{-1} \text{ protein}$) with oligomycin present for liver mitochondria from northern and southern *F. heteroclitus* exposed to control conditions (black bars) or $35 \mu\text{mol l}^{-1}$ palmitate (white bars) and assayed at 15°C. At each acclimation temperature, control and palmitate O_2 consumption values were compared at the membrane potential demonstrating the greatest effect of palmitate: (A) northern killifish: 5°C at 164 mV, 15°C at 165 mV and 25°C at 158 mV; (B) southern killifish: 5°C at 151 mV, 15°C at 142 mV and 25°C at 145 mV. An asterisk indicates significant differences between treatments at a given acclimation temperature and membrane potential as determined by a *t*-test. Data are means \pm s.e.m. ($n=6-7$ for each group).

What are the mRNA expression patterns of UCP isoforms in both subspecies with thermal acclimation?

To investigate whether UCPs could be involved in regulating proton leak in killifish, we first characterized the complement of UCP isoforms present in this species. The phylogenetic relationships between the *Ucp* isoform gene sequences from fish and tetrapod species support the existence of a core *Ucp* family consisting of the closely related *Ucp1*, *Ucp2* and *Ucp3*, with *Ucp5* being less closely related (Fig. 1) (Jastroch et al., 2005; Mark et al., 2006; Tine et al., 2012; Tseng et al., 2011; Wen et al., 2015). However, our ability to discriminate among these families was limited (as indicated by the low bootstrap values on the branches for *Ucp1*, *Ucp2* and *Ucp3*; Fig. 1), which is most likely due to high similarity in the sequences of the members of the core *Ucp* family (Hughes and Criscuolo, 2008). In addition, a fish-specific isoform (*Ucp3L*) was also identified in *F. heteroclitus* and was shown to be most closely related to the fish *Ucp3* isoform gene sequence. *Ucp3L* has previously been identified in other studies as a fish-specific *Ucp* isoform that is believed to be a product of the teleost genome duplication event (Tine et al., 2012; Wen et al., 2015). This isoform has been independently lost in several fish species, but is present in several others (Tine et al., 2012). We were unable to identify *Ucp4* in the genome of *F. heteroclitus*, but it has previously been identified in zebrafish and cave fish (Wen et al., 2015; Tseng et al., 2011), suggesting that it is present in at least some fish species. At present, the killifish genome is not entirely complete, and thus this isoform may be present in one of the unsequenced regions. Alternatively, this isoform may have been lost from the killifish genome.

Ucp mRNA displayed tissue-specific expression patterns, consistent with what is known in other species (Fig. 2 and Figs S3–S6). In mammals, *Ucp1* is found in BAT (Nicholls and Locke, 1984; Nicholls, 2001), whereas in fish, *Ucp1* has been found primarily in the liver, where it has the highest expression relative to the other isoforms (Jastroch et al., 2005; Wen et al., 2015). This is also the case in *F. heteroclitus* (Fig. 2C), although it was also present at intermediate levels in gill tissue (Fig. 2B). *Ucp3* is known to be a skeletal-muscle-specific isoform across species from fish to mammals (Boss et al., 1997; dos Santos et al., 2013b; Vidal-Puig et al., 1997), and it is also found in *F. heteroclitus* at the highest levels in skeletal muscle (Fig. 2D). The fish-specific isoform, *Ucp3L*, has been identified in several other fish species, but its tissue distribution has not been fully characterized (Tine et al., 2012; Wen et al., 2015). Here, we show that *Ucp3L* is primarily expressed in gill tissue in *F. heteroclitus* (Fig. 2B). Gill tissue displayed the most diversity in *Ucp* isoform expression, potentially indicating that the different UCP isoforms may play separate functional roles or may differ by cell types even within a tissue. *Ucp5* was most highly expressed in the brain (Fig. 2B), and this has also been demonstrated in zebrafish (Tseng et al., 2011). The consistency of killifish *Ucp* mRNA expression with that of other species further indicates that the tissue-specific expression patterns of the *Ucp* isoforms are conserved and are likely functionally important.

The effects of thermal acclimation on *Ucp* mRNA expression patterns differed depending on isoform, tissue and subspecies (Fig. 3 and Figs S3–S6). This may be indicative of each isoform having a different functional role in response to thermal acclimation and this role varying depending on the tissue and subspecies being investigated. One possible mechanism that could account for differences in gene expression among acclimation temperatures could be differences in mitochondrial volume density with thermal acclimation. Fangue et al. (2009a,b) and Chung et al. (2018) provided some evidence that there may be an increase in

mitochondrial amount or volume density following cold exposure in liver tissue from northern killifish. Similarly, Dhillion and Schulte (2011) detected increases in mitochondrial volume density in the muscle of northern killifish following cold acclimation. However, if a change in mitochondrial volume density was the only factor influencing the level of *Ucp* mRNA expression, it would be expected that all isoforms would change in a similar manner correlating to changes in mitochondrial volume density. In contrast, we found that the patterns of expression of different *Ucp* isoforms were not the same within a single tissue, suggesting that single factor such as a change in mitochondrial volume density is unlikely to drive all of the observed *Ucp* mRNA expression patterns. Instead, we hypothesize that the different *Ucp* isoforms are likely regulated through different transcriptional regulatory programs.

Ucp mRNA expression changes more in northern killifish liver mitochondria with thermal acclimation than it does in southern killifish (Fig. 3 and Figs S3–S6). This suggests that northern killifish have an enhanced capacity to respond to thermal acclimation. Although both subspecies experience similar variation in temperature throughout the seasons, the range of temperatures at the northern latitudes is colder than that at the southern latitudes (Fangue et al., 2006; Schulte, 2007). Thus animals or populations that experience winter cold may require greater plasticity of thermal responses than those that experience overall warmer temperatures. Further investigation is required to determine whether this is a general pattern. Overall, the patterns we observe in *Ucp* mRNA expression are consistent with the hypothesis that northern killifish have greater plasticity in mitochondrial function compared with southern killifish.

What are the effects of thermal acclimation on mitochondrial function in northern and southern killifish?

In addition to changes in *Ucp* mRNA expression, changes in mitochondrial function with thermal acclimation were observed in northern, but not southern, killifish liver mitochondria. This provides additional evidence that there are differences in the ability of these subspecies to respond to thermal change. Liver mitochondria from cold-acclimated northern killifish exhibited increases in ADP-phosphorylating respiration (state III; Fig. 4A), maximal ETS capacity measured as FCCP-stimulated respiration (Fig. 4C), mitochondrial coupling (RCRs, FCCP-stimulated respiration and P/O; Figs 4D and 5) and proton conductance (Fig. 6A,D). These changes in northern killifish liver mitochondria are consistent with compensation for decreased enzyme activity following prolonged cold exposure, as has been observed in other fish species (Guderley, 2004; dos Santos et al., 2013a; St-Pierre et al., 1998; Chung et al., 2018). The potential for cold compensation has previously been detected in another population of northern *F. heteroclitus* (Chung and Schulte, 2015; Chung et al., 2018), collectively supporting a role for increases in respiratory capacity as a compensatory mechanism in the northern subspecies of killifish. Unlike northern killifish liver mitochondria, we did not detect cold compensation in southern killifish liver mitochondria. However, Chung et al. (2018) found that an increase in mitochondrial respiratory capacity following cold acclimation in both northern and southern killifish. A possible explanation for this discrepancy is that Chung et al. (2018) provided liver mitochondria with either complex I or a mixture of complex I and complex II substrates, whereas in our study, only complex II substrates were provided. This suggests that there may be differences between the subspecies in the ability to change different components of mitochondrial physiology in response to thermal acclimation.

Cold acclimation caused a pronounced shift in proton leak kinetics in northern killifish, such that northern killifish had increased proton conductance, as represented by increased state II (leak) O_2 consumption rates and changes in the shape and position of the proton leak kinetic curve, following acclimation to 5°C (Fig. 6A,D). In contrast, proton leak kinetics did not differ significantly with thermal acclimation in southern killifish (Fig. 6B,D). Northern fish at 5°C also exhibited greater initial $\Delta\Psi_m$ under state II conditions (Fig. 6A), suggesting that in addition to an increase in proton leak, there was also an increase in substrate oxidation or ETS capacity following cold acclimation. In contrast, there was no evidence of cold compensation in respiratory capacity, proton leak or coupling in southern killifish. When considered together, the increase in proton leak (Fig. 6A,D) along with the P/O ratios (Fig. 5), state IV respiration rates (Fig. 4B) and RCRs (Fig. 4C) suggest that liver mitochondria from cold-acclimated northern fish exhibit increases in proton leak, mitochondrial capacity and ADP-phosphorylating capacity following cold acclimation, whereas liver mitochondria from southern killifish do not demonstrate this effect.

Following acclimation to 25°C, southern killifish had greater P/O ratios than northern killifish, indicating that mitochondria from southern killifish are more efficient than those from northern killifish following warm acclimation (Fig. 5), suggestive of improved performance in response to warm acclimation in the putatively warm-adapted subspecies. However, there were no differences between the subspecies in leak respiration or mitochondrial coupling (Fig. 4B,D). This apparent discrepancy suggests that there may be differences between the subspecies in thermal acclimation responses of different ETS components and in mitochondrial coupling under non-phosphorylating (state IV) or phosphorylating (state III) conditions and provides a clear example of the difficulty of interpreting measures of state IV respiration and RCR values.

Taken together, these results suggest that northern, but not southern, killifish recruit substantial changes in mitochondrial capacity and proton leak in response to cold acclimation, which supports a role for putative local adaptation in thermal responses. The effects of cold acclimation on mitochondrial capacity and proton leak in northern killifish contrast against cold-acclimation responses in other ectotherms (Jastroch et al., 2007; Trzcionka et al., 2008). Indeed, Trzcionka et al. (2008) and Jastroch et al. (2007) observed a marked decrease in proton conductance in response to cold acclimation in liver mitochondria from cane toads (*Bufo marinus*) and common carp (*Cyprinus carpio*), respectively. Both studies interpreted the decrease in proton leak as a mechanism to increase mitochondrial efficiency as an energy-saving mechanism related to cold-induced metabolic depression. In contrast, in northern killifish, we observed an increase in mitochondrial capacity and proton conductance in the cold, suggesting a pattern of cold compensation. Similarly, in goldfish, dos Santos et al. (2013a) detected increases in state IV respiration rate in skeletal muscle mitochondria with cold acclimation, suggesting increases in proton leak in the cold. However, dos Santos et al. (2013a) did not characterize proton leak kinetic curves to accurately estimate proton leak at a common $\Delta\Psi_m$ and were thus unable to disentangle the effects of changes in proton leak from changes in substrate oxidation (Divakaruni and Brand, 2011). Interestingly, in goldfish, state III and state IV respiration rates increased in parallel in response to cold acclimation, resulting in no change in RCR (dos Santos et al., 2013a), whereas in northern killifish, we observed a greater change in state III respiration compared with state IV respiration, resulting

in an increase in RCR following cold acclimation. This indicates that ectotherms may adjust both mitochondrial substrate oxidation and proton leak in different ways in order to cope with the effects of long-term cold exposure.

Is there a correlation between *Ucp* mRNA expression and fatty-acid-induced uncoupling in killifish liver mitochondria?

We investigated mitochondrial responses to the presence of the fatty acid palmitate in order to demonstrate a putative functional role for UCPs in modulating mitochondrial proton leak with thermal acclimation. We predicted that fatty-acid-induced uncoupling would be greatest in northern killifish at lower temperatures as *Ucp1* was more highly expressed in liver of northern killifish than in southern killifish at all acclimation temperatures, and decreased greatly in both subspecies at an acclimation temperature of 25°C (Fig. 3A). Consistent with our prediction, fatty-acid-induced uncoupling from isolated killifish liver mitochondria was only observed in northern killifish mitochondria at 5 and 15°C (Figs 7 and 8). These data indicate that the northern subspecies, which experiences colder habitat temperatures, may have a greater capacity adjust mitochondrial function following cold exposure, and that one component contributing to this response may involve the regulation of *Ucp1*.

A notable finding from our work is that we were not able to inhibit fatty-acid-induced uncoupling using classic UCP inhibitors such as GDP or GTP. The effectiveness of UCP inhibition by different purine nucleotides *in vitro* is still debated (e.g. Woyda-Ploszczyca and Jarmuszkiewicz, 2014), and in some scenarios, such as with goldfish UCP3 in skeletal muscle (dos Santos et al., 2013b) and lamprey UCP (Wang et al., 2010), inhibition by purine nucleotides cannot be induced. There are several possibilities as to why purine nucleotides did not inhibit fatty-acid-induced uncoupling. Firstly, the structure of killifish UCP1 may prevent the binding of purine nucleotides. The amino acid sequence hypothesized to be associated with purine nucleotide binding (amino acids 261–269; Bouillaud et al., 1994) differs by two amino acids between mammalian and killifish genomes. Phe267 is Tyr267 in the killifish UCP1 and Ala264 is Thr264 in the killifish UCP1 (NCBI killifish genome, *Fundulus heteroclitus*-3.0.2, GCF_000826765.1, annotation release 101). Although the importance of the Ala→Thr substitution has not been investigated, there is some evidence that the Phe→Tyr substitution does not appear to alter UCP function (Bouillaud et al., 1994). Other amino acids that may be involved in UCP purine nucleotide binding include three Arg residues (Modrianský et al., 1997) of which killifish have all three. Another possibility is that any observed fatty-acid-induced uncoupling is not due to UCPs at all and is a result of another effect palmitate has on the mitochondrial membrane (Ibarguren et al., 2014; Zavodnik et al., 1996). All of the functional assays (including those with palmitate addition) were performed in the presence of Cat, an ANT inhibitor. However, the efficacy of Cat for inhibiting the ANT was not directly tested and therefore we cannot fully rule out the potential effects of ANT-mediated proton leak. Preliminary analyses in northern fish acclimated to 15°C indicated that ANT may contribute to approximately 20% of leak respiration. We have yet to test for the possibility that ANT may contribute more substantially to the modulation of mitochondrial proton leak in southern killifish or in northern killifish at other acclimation temperatures.

If the moderate fatty-acid-induced uncoupling seen here is due to UCPs, this may suggest that northern killifish liver mitochondria have a greater capacity to uncouple through UCPs following acclimation to colder temperatures (5 and 15°C). Other studies in

fish have suggested that increases in uncoupling in the cold may occur to mitigate oxidative damage (e.g. Jastroch et al., 2007). Compensatory increases in mitochondrial function, plus the increased susceptibility of highly saturated fatty acids to lipid peroxidation in the cold (Grim et al., 2010), may be a reason that UCP mRNA expression and possibly uncoupling capacity is greater in the northern subspecies than in the southern subspecies, particularly following cold acclimation. Although there is no significant fatty-acid-induced uncoupling evident in the northern killifish liver mitochondria following acclimation to 25°C or in the southern killifish mitochondria at any acclimation temperature, this may be due to intraspecific or temperature-dependent differences in antioxidant mechanisms. ROS metabolism is a product of both synthesis and detoxification of free radicals. Thus, if fish do not compensate for an increase in ROS synthesis, they may be able to mitigate oxidative damage through an increase in detox pathways (e.g. dismutases and reductases; Sheng et al., 2014). It is possible that different antioxidant mechanisms may be upregulated at different times during the mitochondrial thermal response and that UCPs may be involved earlier in the acclimation process. Changes in mRNA expression and the function of UCPs have been seen to change in as little as a few hours in some species (e.g. Tseng et al., 2011) and have been shown after as long as 2 months in others (e.g. Mark et al., 2006). Further investigation into the time-course responses of potential antioxidant mechanisms, including UCPs and ANT, could elucidate the importance of changes in mitochondrial function in response to thermal change.

Conclusions

We have shown that thermal acclimation has substantial effects on mitochondrial coupling and proton leak in northern, but not southern, *F. heteroclitus*. UCPs, proteins that can contribute to proton leak, were also shown to differ in mRNA expression following thermal acclimation in both subspecies, although this only corresponded to modest differences in fatty-acid-induced uncoupling capacity. This suggests that although there are substantial differences between the subspecies in mitochondrial coupling and proton leak, these differences are not solely due to UCPs. Overall, we provide evidence that mitochondria from putatively cold-adapted northern killifish have a more plastic response to thermal acclimation than mitochondria from southern killifish, particularly in response to cold acclimation. This suggests that alterations to mitochondrial function associated with putative thermal adaptation may be important in determining organismal responses to changing environmental temperature.

Acknowledgements

Thanks to Aquatic Research Organisms for collection of northern killifish.

Competing interests

The authors declare no competing or financial interests.

Author contributions

Conceptualization: H.J.B., D.J.C., P.M.S.; Methodology: H.J.B., D.J.C., P.M.S.; Validation: H.J.B.; Formal analysis: H.J.B., D.J.C.; Investigation: H.J.B.; Resources: P.M.S.; Data curation: H.J.B., P.M.S.; Writing - original draft: H.J.B.; Writing - review & editing: H.J.B., D.J.C., P.M.S.; Visualization: H.J.B.; Supervision: D.J.C., P.M.S.; Project administration: P.M.S.; Funding acquisition: P.M.S.

Funding

Funding was provided in the form of a National Science and Engineering Research Council of Canada (NSERC) Discovery Grant to P.M.S., an NSERC Canada Graduate Scholarship – Master's to H.J.B., and an NSERC Canada Graduate Scholarship – Doctoral to D.J.C.

Supplementary information

Supplementary information available online at <http://jeb.biologists.org/lookup/doi/10.1242/jeb.186320.supplemental>

References

- Abele, D., Heise, K., Pörtner, H. O. and Puntarulo, S. (2002). Temperature-dependence of mitochondrial function and production of reactive oxygen species in the intertidal mud clam *Mya arenaria*. *J. Exp. Biol.* **205**, 1831-1841.
- Affourtit, C., Wong, H. S. and Brand, M. D. (2018). Measurement of proton leak in isolated mitochondria. In *Mitochondrial Bioenergetics. Methods in Molecular Biology*, Vol. 1782 (ed. C. Palmeira and A. Moreno), pp.157-170. New York, NY: Humana Press.
- Bishop, T. and Brand, M. D. (2000). Processes contributing to metabolic depression in hepatopancreas cells from the snail *Helix aspersa*. *J. Exp. Biol.* **203**, 3603-3612.
- Boss, O., Samec, S., Paoloni-Giacobino, A., Rossier, C., Dulloo, A., Seydoux, J., Muzzin, P. and Giacobino, J.-P. (1997). Uncoupling protein-3: a new member of the mitochondrial carrier family with tissue-specific expression. *FEBS Lett.* **408**, 39-42.
- Bouillaud, F., Arechaga, I., Petit, P. X., Raimbault, S., Levi-Meyreuis, C., Casteilla, L., Laurent, M., Rial, E. and Ricquier, D. (1994). A sequence related to a DNA recognition element is essential for the inhibition by nucleotides of proton transport through the mitochondrial uncoupling protein. *EMBO J.* **13**, 1990-1997.
- Bradford, M. M. (1976). A rapid and sensitive method for the quantitation of microgram quantities of protein utilizing the principle of protein-dye binding. *Anal. Biochem.* **72**, 248-254.
- Brand, M. D. (2005). The efficiency and plasticity of mitochondrial energy transduction. *Biochem. Soc. Trans.* **33**, 897-904.
- Brand, M. D. and Esteves, T. C. (2005). Physiological functions of the mitochondrial uncoupling proteins UCP2 and UCP3. *Cell Metab.* **2**, 85-93.
- Brand, M. D., Couture, P., Else, P. L., Withers, K. W. and Hulbert, A. J. (1991). Evolution of energy metabolism. Proton permeability of the inner membrane of liver mitochondria is greater in a mammal than in a reptile. *Biochem. J.* **275**, 81-86.
- Brand, M. D., Couture, P. and Hulbert, A. J. (1994). Liposomes from mammalian liver mitochondria are more polyunsaturated and leakier to protons than those from reptiles. *Comp. Biochem. Physiol. B* **108**, 181-188.
- Chance, B. and Williams, G. R. (1955). Respiratory enzymes in oxidative phosphorylation I. Kinetics of oxygen utilization. *J. Biol. Chem.* **217**, 383-393.
- Chung, D. J. and Schulte, P. M. (2015). Mechanisms and costs of mitochondrial thermal acclimation in a eurythermal killifish (*Fundulus heteroclitus*). *J. Exp. Biol.* **218**, 1621-1631.
- Chung, D. J., Bryant, H. J. and Schulte, P. M. (2017). Thermal acclimation and subspecies-specific effects on heart and brain mitochondrial performance in a eurythermal teleost (*Fundulus heteroclitus*). *J. Exp. Biol.* **220**, 1459-1471.
- Chung, D. J., Sparagna, G. C., Chicco, A. J. and Schulte, P. M. (2018). Patterns of mitochondrial membrane remodeling parallel functional adaptations to thermal stress. *J. Exp. Biol.* **221**, jeb174458.
- Dahlhoff, E. A. and Somero, G. N. (1993). Effects of temperature on mitochondria from abalone (genus *Haliotis*): adaptive plasticity and its limits. *J. Exp. Biol.* **185**, 151-168.
- Davis, L. M., Rho, J. M. and Sullivan, P. G. (2008). UCP-mediated free fatty acid uncoupling of isolated cortical mitochondria from fasted animals: correlations to dietary modulations. *Epilepsia* **8**, 117-119.
- Dhillon, R. S. and Schulte, P. M. (2011). Intraspecific variation in the thermal plasticity of mitochondria in killifish. *J. Exp. Biol.* **214**, 3639-3648.
- Divakaruni, A. S. and Brand, M. D. (2011). The regulation and physiology of mitochondrial proton leak. *Physiology (Bethesda)* **26**, 192-205.
- dos Santos, R. S., Galina, A. and Da-Silva, W. S. (2013a). Cold acclimation increases mitochondrial oxidative capacity without inducing mitochondrial uncoupling in goldfish white skeletal muscle. *Biol. Open* **2**, 82-87.
- dos Santos, R. S., Peçanha, F. L. M. and Da-Silva, W. S. (2013b). Functional characterization of an uncoupling protein in goldfish white skeletal muscle. *J. Bioenerg. Biomembr.* **45**, 243-251.
- Edgar, R. C. (2004). MUSCLE: multiple sequence alignment with high accuracy and high throughput. *Nucleic Acids Res.* **32**, 1792-1797.
- Esteves, T. C. and Brand, M. D. (2005). The reactions catalysed by the mitochondrial uncoupling proteins UCP2 and UCP3. *Biochim. Biophys. Acta* **1709**, 35-44.
- Fangue, N. A., Hofmeister, M. and Schulte, P. M. (2006). Intraspecific variation in thermal tolerance and heat shock protein gene expression in common killifish, *Fundulus heteroclitus*. *J. Exp. Biol.* **209**, 2859-2872.
- Fangue, N. A., Podrabsky, J. E., Crawshaw, L. I. and Schulte, P. M. (2009a). Countergradient variation in temperature preference in populations of killifish *Fundulus heteroclitus*. *Physiol. Biochem. Zool.* **82**, 776-786.
- Fangue, N. A., Richards, J. G. and Schulte, P. M. (2009b). Do mitochondrial properties explain intraspecific variation in thermal tolerance? *J. Exp. Biol.* **212**, 514-522.
- Forstner, H. and Gnaiger, E. (1983). Calculation of equilibrium oxygen concentration. In *Polarographic Oxygen Sensors* (ed. E. Gnaiger and H. Forstner), pp. 321-333. Springer.

- Gnaiger, E.** (2014). *Mitochondrial Pathways of Respiratory Control. An Introduction to OXPHOS Analysis*, 4th edn. pp. 1-80. Innsbruck: MIPNet Publications.
- Gnaiger, E. and Kuznetsov, A. V.** (2002). Mitochondrial respiration at low levels of oxygen and cytochrome *c*. *Biochem. Soc. Trans.* **30**, 252-258.
- Gnaiger, E., Méndez, G. and Hand, S. C.** (2000). High phosphorylation efficiency and depression of uncoupled respiration in mitochondria under hypoxia. *Proc. Natl. Acad. Sci. USA* **97**, 11080-11085.
- Grim, J. M., Miles, D. R. B. and Crockett, E. L.** (2010). Temperature acclimation alters oxidative capacities and composition of membrane lipids without influencing activities of enzymatic antioxidants or susceptibility to lipid peroxidation in fish muscle. *J. Exp. Biol.* **213**, 445-452.
- Guderley, H.** (1990). Functional significance of metabolic responses to thermal acclimation in fish muscle. *Am. J. Physiol.* **259**, R245-R252.
- Guderley, H.** (2004). Metabolic responses to low temperature in fish muscle. *Biol. Rev. Camb. Philos. Soc.* **79**, 409-427.
- Guderley, H. and Johnston, I. A.** (1996). Plasticity of fish mitochondria with thermal acclimation. *J. Exp. Biol.* **199**, 1311-1317.
- Healy, T. M. and Schulte, P. M.** (2012). Thermal acclimation is not necessary to maintain a wide thermal breadth of aerobic scope in the common killifish (*Fundulus heteroclitus*). *Physiol. Biochem. Zool.* **85**, 107-119.
- Healy, T. M., Bryant, H. J. and Schulte, P. M.** (2017). Mitochondrial genotype and phenotypic plasticity of gene expression in response to cold acclimation in killifish. *Mol. Ecol.* **26**, 814-830.
- Hochachka, P. W. and Somero, G. N.** (2002). *Biochemical Adaptation: Mechanism and Process in Physiological Evolution*. Oxford: Oxford University Press.
- Hughes, J. and Criscuolo, F.** (2008). Evolutionary history of the UCP gene family: gene duplication and selection. *BMC Evol. Biol.* **8**, 306.
- Ibarguren, M., López, D. J. and Escribá, P. V.** (2014). The effect of natural and synthetic fatty acids on membrane structure, microdomain organization, cellular functions and human health. *Biochim. Biophys. Acta* **1838**, 1518-1528.
- Iftikar, F. I. and Hickey, A. J. R.** (2013). Do mitochondria limit hot fish hearts? Understanding the role of mitochondrial function with heat stress in *Notolabrus celidodus*. *PLoS ONE* **8**, e64120.
- Jastroch, M., Wuertz, S., Kloas, W. and Klingenspor, M.** (2005). Uncoupling protein 1 in fish uncovers an ancient evolutionary history of mammalian nonshivering thermogenesis. *Physiol. Genomics* **22**, 150-156.
- Jastroch, M., Buckingham, J. A., Helwig, M., Klingenspor, M. and Brand, M. D.** (2007). Functional characterisation of UCP1 in the common carp: uncoupling activity in liver mitochondria and cold-induced expression in the brain. *J. Comp. Physiol. B* **177**, 743-752.
- Jastroch, M., Divakaruni, A. S., Mookerjee, S., Treberg, J. R. and Brand, M. D.** (2010). Mitochondrial proton and electron leaks. *Essays Biochem.* **47**, 53-67.
- Jastroch, M., Hirschberg, V. and Klingenspor, M.** (2012). Functional characterization of UCP1 in mammalian HEK293 cells excludes mitochondrial uncoupling artefacts and reveals no contribution to basal proton leak. *Biochim. Biophys. Acta* **1817**, 1660-1670.
- Klingenspor, M. and Huang, S.-G.** (1999). Structure and function of the uncoupling protein from brown adipose tissue. *Biochim. Biophys. Acta* **1415**, 271-296.
- Kneib, R. T. and Stiven, A. E.** (1978). Growth, reproduction, and feeding of *Fundulus heteroclitus* (L.) on a North Carolina salt marsh. *J. Exp. Mar. Biol. Ecol.* **31**, 121-140.
- Kraffe, E., Marty, Y. and Guderley, H.** (2007). Changes in mitochondrial oxidative capacities during thermal acclimation of rainbow trout *Oncorhynchus mykiss*: roles of membrane proteins, phospholipids and their fatty acid compositions. *J. Exp. Biol.* **210**, 149-165.
- Lannig, G., Storch, D. and Pörtner, H.-O.** (2005). Aerobic mitochondrial capacities in Antarctic and temperate eelpout (Zoarcidae) subjected to warm versus cold acclimation. *Polar Biol.* **28**, 575-584.
- Mark, F. C., Lucassen, M. and Pörtner, H. O.** (2006). Thermal sensitivity of uncoupling protein expression in polar and temperate fish. *Comp. Biochem. Physiol. D* **1**, 365-374.
- McBryan, T. L., Healy, T. M., Haakons, K. L. and Schulte, P. M.** (2016). Warm acclimation improves hypoxia tolerance in *Fundulus heteroclitus*. *J. Exp. Biol.* **219**, 474-484.
- Modrianský, M., Murdza-Inglis, D. L., Patel, H. V., Freeman, K. B. and Garlid, K. D.** (1997). Identification by site-directed mutagenesis of three arginines in uncoupling protein that are essential for nucleotide binding and inhibition. *J. Biol. Chem.* **272**, 24759-24762.
- Moyes, C. D., Buck, L. T. and Hochachka, P. W.** (1988). Temperature effects on pH of mitochondria isolated from carp red muscle. *Am. J. Physiol.* **254**, R611-R615.
- Murakami, M., Ohi, M., Ishikawa, S., Shirai, M., Horiguchi, H., Nishino, Y. and Funaba, M.** (2015). Adaptive expression of uncoupling protein 1 in the carp liver and kidney in response to changes in ambient temperature. *Comp. Biochem. Physiol. A* **185**, 142-149.
- Murphy, M. P.** (1989). Slip and leak in mitochondrial oxidative phosphorylation. *Biochim. Biophys. Acta* **977**, 123-141.
- Nicholls, D. G.** (1977). The effective proton conductance of the inner membrane of mitochondria from brown adipose tissue. Dependency on proton electrochemical potential gradient. *Eur. J. Biochem.* **77**, 349-356.
- Nicholls, D. G.** (2001). A history of UCPI. *Biochem. Soc. Trans.* **29**, 751-755.
- Nicholls, D. G. and Locke, R. M.** (1984). Thermogenic mechanisms in brown fat. *Physiol. Rev.* **61**, 1-64.
- Porter, R. K. and Brand, M. D.** (1993). Body mass dependence of H⁺ leak in mitochondria and its relevance to metabolic rate. *Nature* **362**, 628-630.
- Pörtner, H.** (2001). Climate change and temperature-dependent biogeography: oxygen limitation of thermal tolerance in animals. *Naturwissenschaften* **88**, 137-146.
- Richieri, G. V., Anel, A. and Kleinfeld, A. M.** (1993). Interactions of long-chain fatty acids and albumin: determination of free fatty acid levels using the fluorescent probe ADIFAB. *Biochemistry* **32**, 7574-7580.
- Rolfe, D. F. S., Newman, J. M. B., Buckingham, J. A., Clark, M. G. and Brand, M. D.** (1999). Contribution of mitochondrial proton leak to respiration rate in working skeletal muscle and liver and to SMR. *Am. J. Physiol.* **276**, C692-C699.
- Rousset, S., Alves-Guerra, M.-C., Mozo, J., Miroux, B., Cassard-Doulcier, A.-M., Bouillaud, F. and Riquier, D.** (2004). The biology of mitochondrial uncoupling proteins. *Diabetes* **53**, S130-S135.
- Salin, K., Auer, S. K., Rey, B., Selman, C. and Metcalfe, N. B.** (2015). Variation in the link between oxygen consumption and ATP production, and its relevance for animal performance. *Proc. R. Soc. B* **282**, 20151028.
- Samartsev, V. N., Smirnov, A. V., Zeldi, I. P., Markova, O. V., Mokhova, E. N. and Skulachev, V. P.** (1997). Involvement of aspartate/glutamate antiporter in fatty acid-induced uncoupling of liver mitochondria. *Biochim. Biophys. Acta* **1319**, 251-257.
- Schulte, P. M.** (2007). Responses to environmental stressors in an estuarine fish: interacting stressors and the impacts of local adaptation. *J. Therm. Biol.* **32**, 152-161.
- Shabalina, I. G., Jacobsson, A., Cannon, B. and Nedergaard, J.** (2004). Native UCP1 displays simple competitive kinetics between the regulators purine nucleotides and fatty acids. *J. Biol. Chem.* **279**, 38236-38248.
- Sheng, Y., Abreu, I. A., Cabelli, D. E., Maroney, M. J., Miller, A.-F., Teixeira, M. and Valentine, J. S.** (2014). Superoxide dismutases and superoxide reductases. *Chem. Rev.* **114**, 3854-3918.
- St-Pierre, J., Charest, P.-M. and Guderley, H.** (1998). Relative contribution of quantitative and qualitative changes in mitochondria to metabolic compensation during seasonal acclimatisation of rainbow trout *Oncorhynchus mykiss*. *J. Exp. Biol.* **201**, 2961-2970.
- Strobel, A., Graeve, M., Poertner, H. O. and Mark, F. C.** (2013). Mitochondrial acclimation capacities to ocean warming and acidification are limited in the Antarctic nototheniid fish, *Notothenia rossii* and *Lepidonotothen squamifrons*. *PLoS ONE* **8**, e68865.
- Tine, M., Kuhl, H., Jastroch, M. and Reinhardt, R.** (2012). Genomic characterization of the European sea bass *Dicentrarchus labrax* reveals the presence of a novel uncoupling protein (UCP) gene family member in the teleost fish lineage. *BMC Evol. Biol.* **12**, 62.
- Trzcionka, M., Withers, K. W., Klingenspor, M. and Jastroch, M.** (2008). The effects of fasting and cold exposure on metabolic rate and mitochondrial proton leak in liver and skeletal muscle of an amphibian, the cane toad *Bufo marinus*. *J. Exp. Biol.* **211**, 1911-1918.
- Tseng, Y.-C., Chen, R.-D., Lucassen, M., Schmidt, M. M., Dringen, R., Abele, D. and Hwang, P.-P.** (2011). Exploring uncoupling proteins and antioxidant mechanisms under acute cold exposure in brains of fish. *PLoS ONE* **6**, e18180.
- van den Thillart, G. and Modderkolk, J.** (1978). The effect of acclimation temperature on the activation energies of state III respiration and on the unsaturation of membrane lipids of goldfish mitochondria. *Biochim. Biophys. Acta* **510**, 38-51.
- Vidal-Puig, A., Solanes, G., Grujic, D., Flier, J. S. and Lowell, B. B.** (1997). UCP3: an uncoupling protein homologue expressed preferentially and abundantly in skeletal muscle and brown adipose tissue. *Biochem. Biophys. Res. Commun.* **235**, 79-82.
- Wang, C., Sun, G., Chen, K., Lv, Z., Peng, S., Jiang, X., Xiang, Y. and Zhang, C.** (2010). Molecular cloning of lamprey uncoupling protein and assessment of its uncoupling activity using a yeast heterologous expression system. *Mitochondrion* **10**, 54-61.
- Wen, Z.-Y., Liang, X.-F., He, S., Li, L., Shen, D. and Tao, Y.-X.** (2015). Molecular cloning and tissue expression of uncoupling protein 1, 2 and 3 genes in Chinese perch (*Siniperca chuatsi*). *Comp. Biochem. Physiol. B* **185**, 24-33.
- Whitehead, A., Roach, J. L., Zhang, S. and Galvez, F.** (2011). Genomic mechanisms of evolved physiological plasticity in killifish distributed along an environmental salinity gradient. *Proc. Natl. Acad. Sci. USA* **108**, 6193-6198.
- Woyda-Ploszczycza, A. M. and Jarmuszkievicz, W.** (2014). Different effects of guanine nucleotides (GDP and GTP) on protein-mediated mitochondrial proton leak. *PLoS ONE* **9**, e98969.
- Woyda-Ploszczycza, A. M. and Jarmuszkievicz, W.** (2017). The conserved regulation of mitochondrial uncoupling proteins: from unicellular eukaryotes to mammals. *Biochim. Biophys. Acta* **1858**, 21-33.
- Zavodnik, I. B., Lapshina, E. A., Palecz, D. and Bryszewska, M.** (1996). The effects of palmitate on human erythrocyte membrane potential and osmotic stability. *Scand. J. Clin. Lab Invest.* **56**, 401-407.

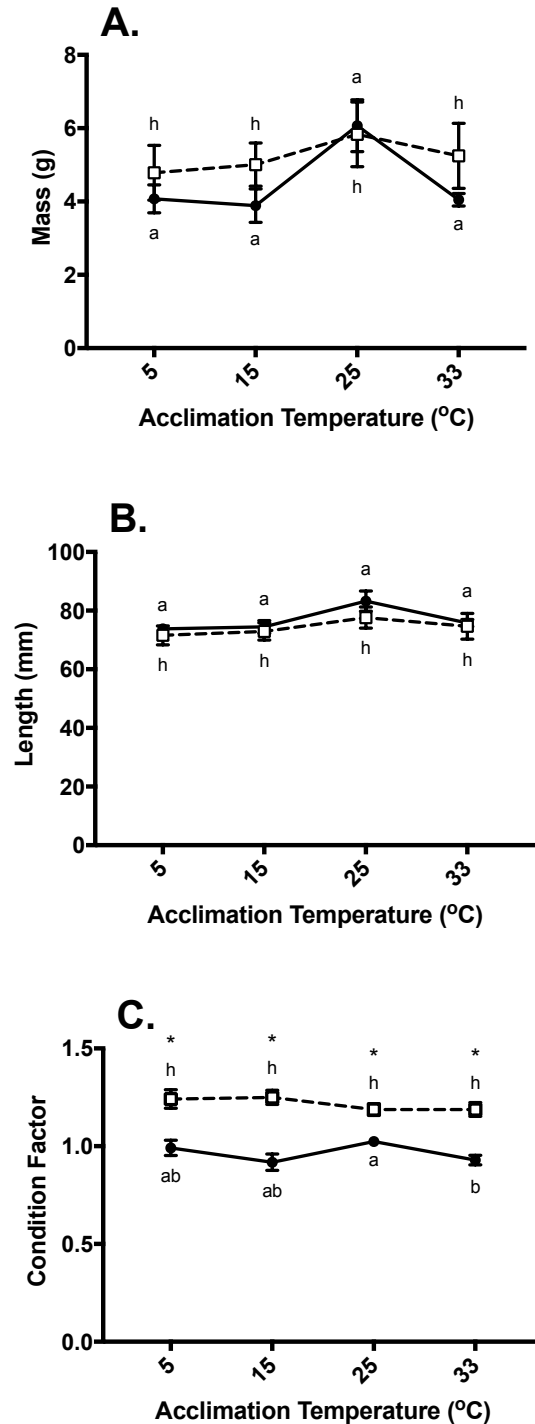


Figure S1. Whole animal measurements for northern (black circles, solid line) and southern (white squares, dashed line) *Fundulus heteroclitus* acclimated to 5, 15, 25, and 33 °C. Data are means \pm s.e.m. (n=8-9 for each group). Shared letters indicate no significant difference as determined by planned comparison *t*-tests followed by FDR correction for mass (A) and condition factor (C). Shared letters indicate no significant difference as determined by Mann-Whitney U rank sum test followed by FDR correction for length (B). An asterisk (*) indicates a significant difference between populations at a given acclimation temperature.

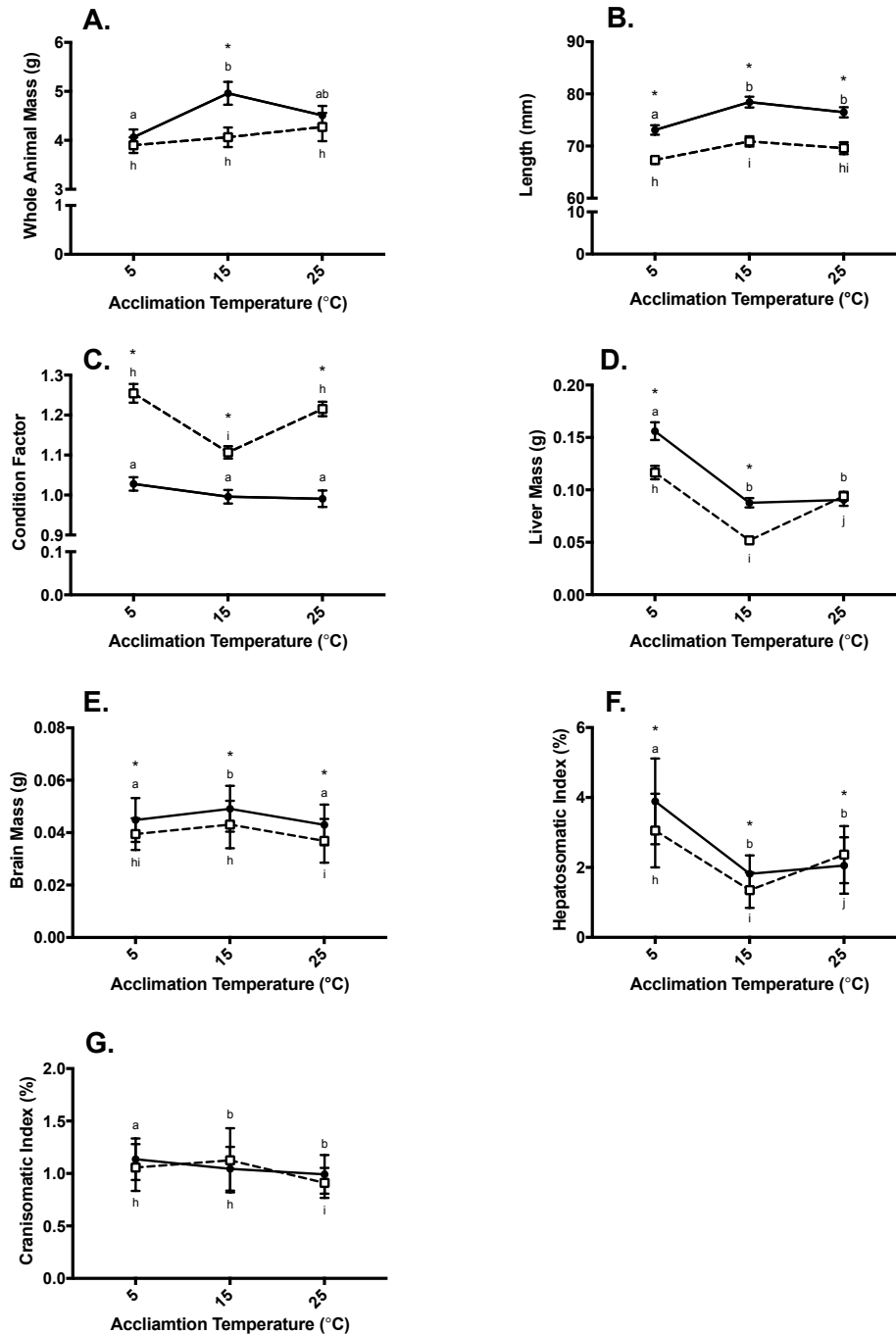


Figure S2. Whole animal measurements for northern (black circles, solid line) and southern (white squares, dashed line) *Fundulus heteroclitus* acclimated to 5, 15 and 25°C. Data are means \pm s.e.m. (n=48-49 for each group). Shared letters indicate no significant difference as determined by planned comparison *t*-tests followed by FDR correction for condition factor (C), liver mass (D), brain mass (E), and hepatosomatic index (F). Shared letters indicate no significant difference as determined by pairwise comparisons using a Mann Whitney U rank sum test followed by FDR correction for whole animal mass (A), length (B), and cranisomatic index (G). An asterisk indicates a significant difference between populations at a given acclimation temperature.

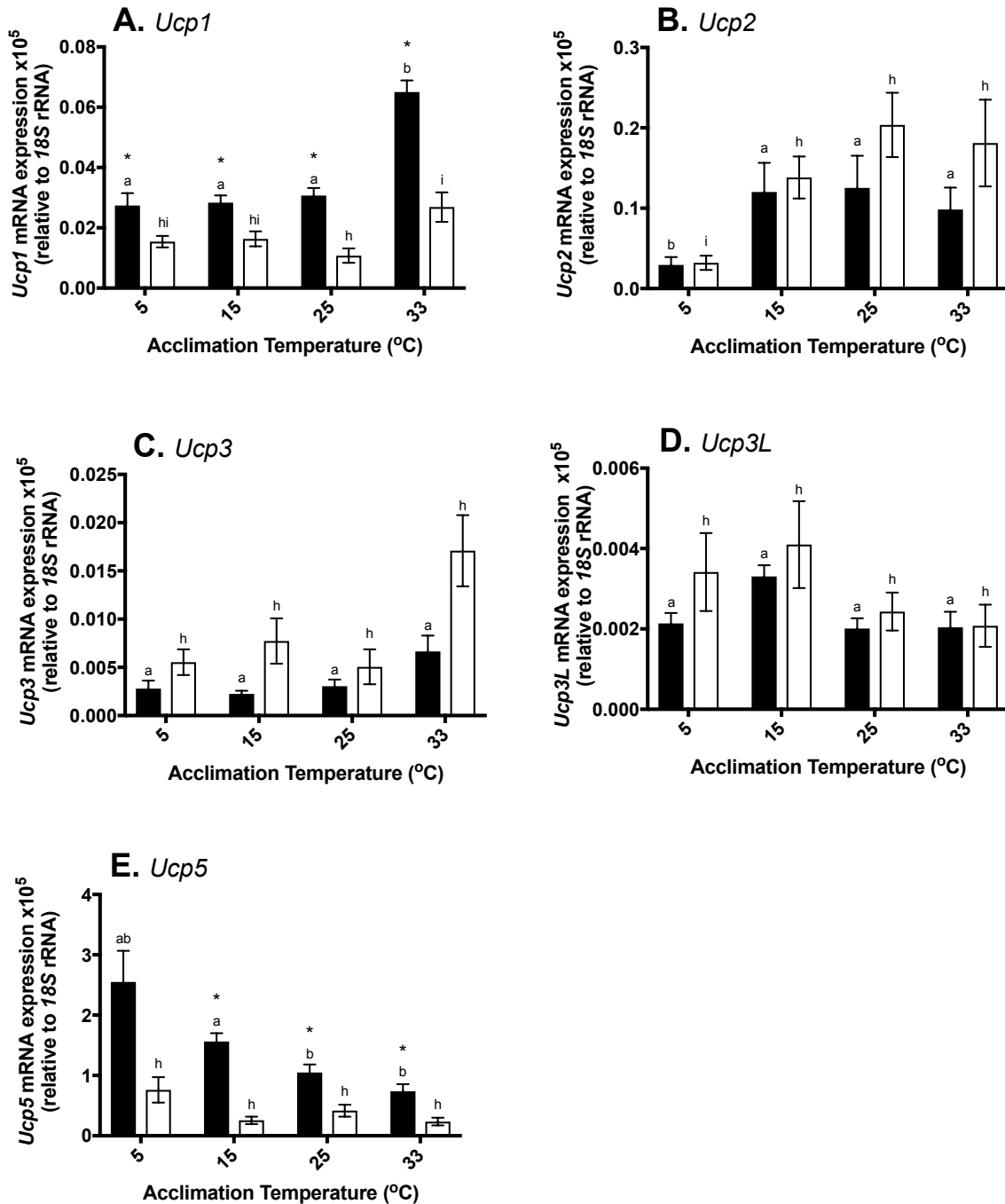


Figure S3. mRNA expression $\times 10^5$ (relative to 18S rRNA) of *Ucp1* (A), *Ucp2* (B), *Ucp3* (C), *Ucp3L* (D), and *Ucp5* (E) in brain tissue from northern (grey bars) and southern (white bars) *Fundulus heteroclitus* across acclimation temperatures (°C). Data are means \pm s.e.m. (n=8-9 for each group). For A-C, letters that differ indicate a significant difference within a population and an asterisk indicates a significant difference between populations at a given acclimation temperature as determined by FDR corrected planned comparisons. For D and E, letters that differ indicate a significant difference within a population and an asterisk indicates a significant difference between populations at a given acclimation temperature as determined by a Mann-Whitney-U rank sum test with FDR corrected *p*-values.

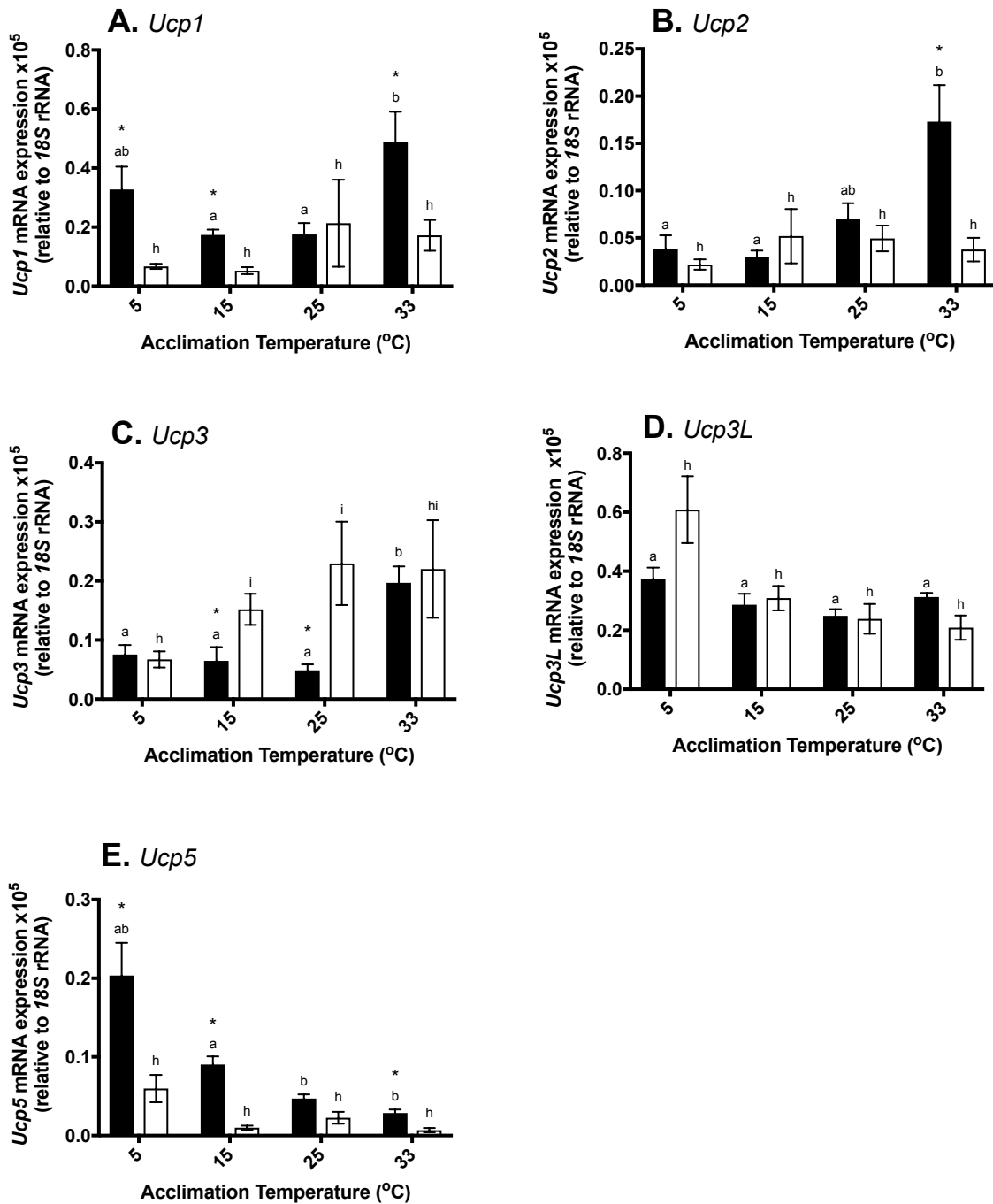


Figure S4. mRNA expression $\times 10^5$ (relative to 18S rRNA) of *Ucp1* (A), *Ucp2* (B), *Ucp3* (C), *Ucp3L* (D), and *Ucp5* (E) in gill tissue from northern (grey bars) and southern (white bars) *Fundulus heteroclitus* across acclimation temperatures (°C). Data are means \pm s.e.m. (n=8-9 for each group). For B-D, letters that differ indicate a significant difference within a population and an asterisk indicates a significant difference between populations at a given acclimation temperature as determined by FDR corrected planned comparisons. For A and E, letters that differ indicate a significant difference within a population and an asterisk indicates a significant difference between populations at a given acclimation temperature as determined by a Mann-Whitney-U rank sum test with FDR corrected *p*-values.

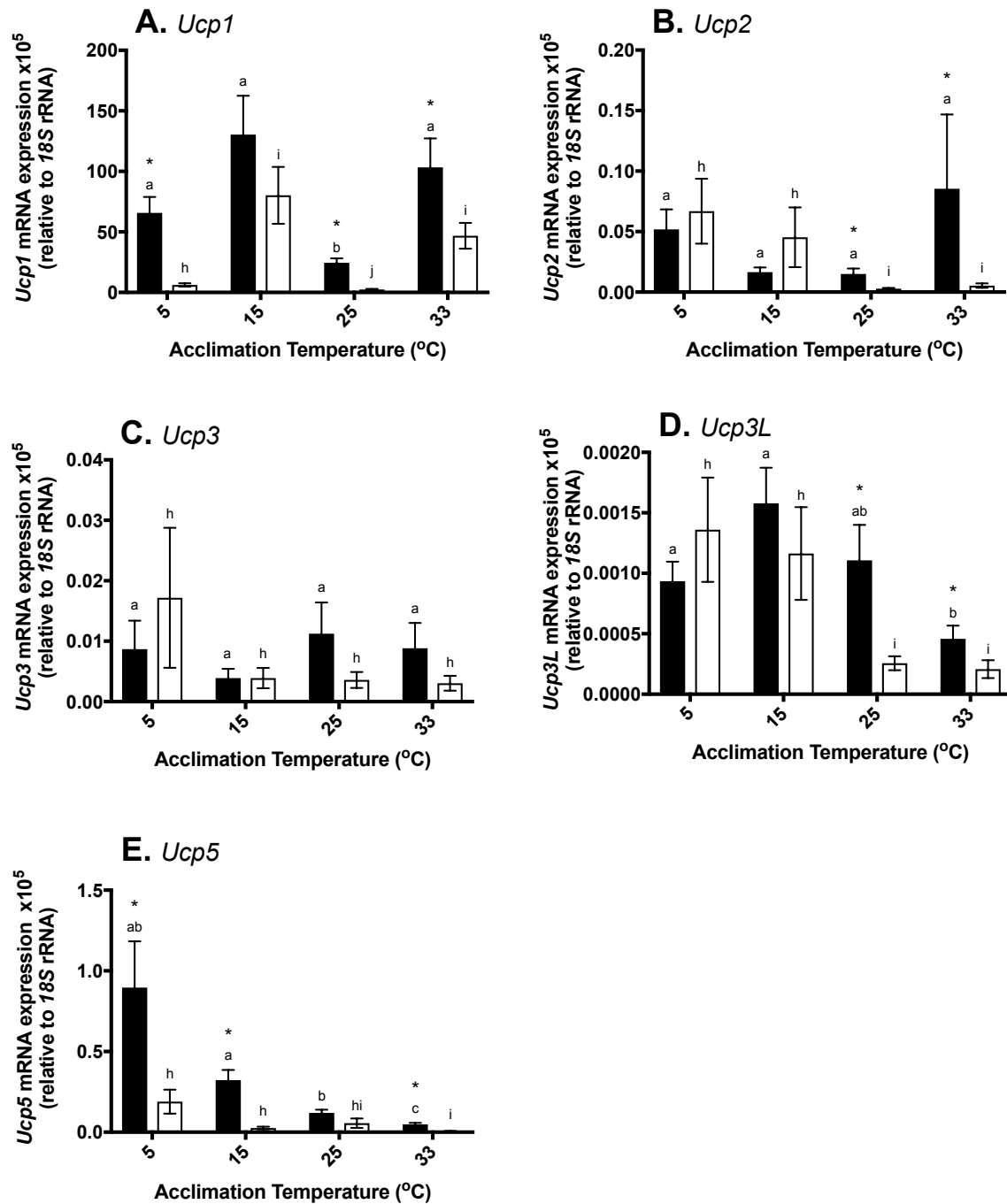


Figure S5. mRNA expression $\times 10^5$ (relative to 18S rRNA) of *Ucp1* (A), *Ucp2* (B), *Ucp3* (C), *Ucp3L* (D), and *Ucp5* (E) in liver tissue from northern (grey bars) and southern (white bars) *Fundulus heteroclitus* across acclimation temperatures (°C). Data are means \pm s.e.m. (n=7-9 for each group). For A, B and D, letters that differ indicate a significant difference within a population and an asterisk indicates a significant difference between populations at a given acclimation temperature as determined by FDR corrected planned comparisons. For C and E, letters that differ indicate a significant difference within a population and an asterisk indicates a significant difference between populations at a given acclimation temperature as determined by a Mann-Whitney-U sum test with FDR corrected *p*-values.

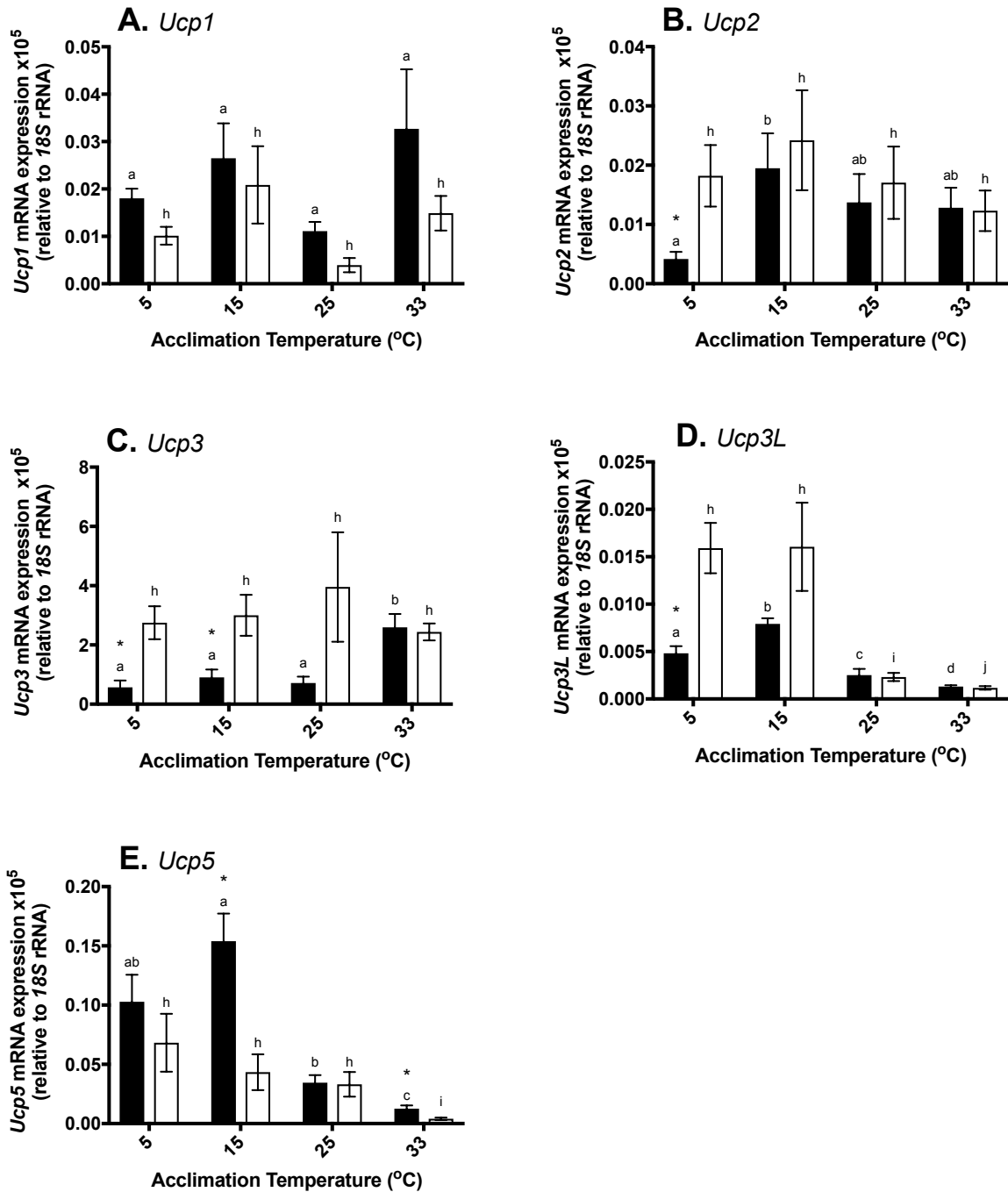


Figure S6. mRNA expression $\times 10^5$ (relative to 18S rRNA) of *Ucp1* (A), *Ucp2* (B), *Ucp3* (C), *Ucp3L* (D), and *Ucp5* (E) in muscle tissue from northern (grey bars) and southern (white bars) *Fundulus heteroclitus* across acclimation temperatures (°C). Data are means \pm s.e.m. (n=8-9 for each group). For A, B and E, letters that differ indicate a significant difference within a population and an asterisk indicates a significant difference between populations at a given acclimation temperature as determined by FDR corrected planned comparisons. For C and D, letters that differ indicate a significant difference within a population and an asterisk indicates a significant difference between populations at a given acclimation temperature as determined by a Mann-Whitney-U sum test with FDR corrected *p*-values.